



CRISTINA GUIMARÃES PEREIRA

**TERMOGRAFIA DE INFRAVERMELHO
APLICADA NA AVALIAÇÃO DA
TRANSFERÊNCIA DE CALOR DURANTE O
CONGELAMENTO DE SOLUÇÃO MODELO DE
SUCO DE FRUTAS EM GRANDES
EMBALAGENS**

**LAVRAS – MG
2017**

CRISTINA GUIMARÃES PEREIRA

**TERMOGRAFIA DE INFRAVERMELHO APLICADA NA AVALIAÇÃO
DA TRANSFERÊNCIA DE CALOR DURANTE O CONGELAMENTO
DE SOLUÇÃO MODELO DE SUCO DE FRUTAS EM GRANDES
EMBALAGENS**

Tese apresentada à Universidade Federal de Lavras, como parte das exigências do Programa de Pós-Graduação em Ciência dos Alimentos, área de concentração em Ciência dos Alimentos, para a obtenção do título de Doutor.

Orientador

Dr. Jaime Vilela de Resende

Coorientador

Dr. Hosahalli S. Ramaswamy

**LAVRAS - MG
2017**

**Ficha catalográfica elaborada pelo Sistema de Geração de Ficha
Catalográfica da Biblioteca Universitária da UFLA, com dados
informados pelo(a) próprio(a) autor(a).**

Pereira, Cristina Guimarães.

Termografia de infravermelho aplicada na avaliação da transferência de calor durante o congelamento de solução modelo de suco de frutas em grandes embalagens / Cristina Guimarães Pereira. - 2016.

88 p.

Orientador(a): Jaime Vilela de Resende.

Tese (doutorado) - Universidade Federal de Lavras, 2016.
Bibliografia.

1. Câmera de infravermelho. 2. Túnel de congelamento. 3. Consumo energético. I. Resende, Jaime Vilela de. II. Título

CRISTINA GUIMARÃES PEREIRA

**TERMOGRAFIA DE INFRAVERMELHO APLICADA NA AVALIAÇÃO
DA TRANSFERÊNCIA DE CALOR DURANTE O CONGELAMENTO
DE SOLUÇÃO MODELO DE SUCO DE FRUTAS EM GRANDES
EMBALAGENS**

**INFRARED THERMOGRAPHY FOR EVALUATION OF HEAT
TRANSFER DURING THE FREEZING OF FRUIT JUICE MODEL
SOLUTIONS IN LARGE CONTAINERS**

Tese apresentada à Universidade Federal de Lavras, como parte das exigências do Programa de Pós-Graduação em Ciência dos Alimentos, área de concentração em Ciência dos Alimentos, para a obtenção do título de Doutor.

APROVADA em 18 de janeiro de 2017.

Dra. Bruna de Souza Nascimento	UFLA
Dr. Jaime Vilela de Resende	UFLA
Dra. Lanamar de Almeida Carlos	UFSJ
Dra. Mônica Elisabeth Torres Prado	UFLA
Dr. Rogério Amaro Gonçalves	IFMG

Dr. Jaime Vilela de Resende
Orientador

Dr. Hosahalli S. Ramaswamy
Coorientador

LAVRAS - MG
2017

Aos meus pais, Edsel e Cleonice, e a minha irmã, Simone, pelo incentivo, amor e exemplo.

Dedico

AGRADECIMENTOS

A Deus, por fazer as coisas certas e no momento certo de nossas vidas, proporcionando-nos conforto e perseverança na realização de nossos sonhos e objetivos.

Ao meu orientador, professor Dr. Jaime Vilela de Resende, pela orientação, paciência, amizade, dedicação e seus ensinamentos, que foram de grande importância para a realização deste trabalho.

Ao meu coorientador no Canadá, professor Dr. Hosahalli S. Ramaswamy, pelos ensinamentos, paciência e contribuição com o trabalho.

Aos meus pais e minha irmã, pelo amor, carinho e estímulo.

A todos do Laboratório de Refrigeração de Alimentos, pelo companheirismo e amizade, especialmente ao colega Tales, pela ajuda indispensável.

Aos colegas de laboratório na McGill University, pela amizade, carinho e paciência.

À Universidade Federal de Lavras (UFLA) e ao Departamento de Ciência dos Alimentos (DCA), por possibilitarem o desenvolvimento deste trabalho.

À McGill University, que me abriu as portas para um novo mundo de aprendizado e possibilitou a complementação deste trabalho.

À Fundação de Amparo à Pesquisa do Estado de Minas Gerais (FAPEMIG), ao Conselho Nacional de Desenvolvimento Científico e Tecnológico (CNPq) e à Coordenação de Aperfeiçoamento de Pessoal de Nível Superior (CAPES), pelo financiamento da pesquisa e a concessão da bolsa de estudos.

RESUMO

Neste trabalho objetivou-se estudar o processo de transferência de calor durante o congelamento de 600 kg de solução modelo de suco de frutas acondicionada em diferentes tipos de embalagens (caixas, baldes e tambores metálicos) e em diferentes configurações, dentro de um túnel de congelamento. Foi mensurada a velocidade do ar em vários pontos dentro de todo o túnel. Para monitoramento e aquisição de perfis de temperatura, termopares foram instalados dentro das soluções, na superfície dos recipientes e no ar de resfriamento. As medidas experimentais do coeficiente de transferência de calor efetivo foram determinadas por meio de um balanço de energia aplicado ao sistema. Para tanto foram utilizados os dados de temperatura obtidos com os termopares e a tecnologia de termografia de infravermelho, sendo possível mapear a distribuição dos coeficientes por toda a superfície. O consumo de energia envolvido em cada arranjo foi avaliado. Os mais altos valores da velocidade do ar ocorreram nos pontos mais elevados dos experimentos, sendo, acima dos tambores, das pilhas de caixas e baldes. Nestes pontos verificou-se a existência de canais preferenciais de fluxo de ar, próximo à porta e ao seu lado oposto. Os valores mais elevados de velocidade do ar foram de $2,85 \text{ m.s}^{-1}$; $2,72 \text{ m.s}^{-1}$ e $2,62 \text{ m.s}^{-1}$, para tambores, caixas e baldes, respectivamente. O movimento da frente de congelamento promoveu-se a partir dos recipientes mais exteriores, indo em direção aos localizados no centro das pilhas e o tempo médio de congelamento foi de 51 horas, para caixas plásticas; 55 horas, para baldes plásticos e 102 horas, para os tambores metálicos. O consumo de energia na configuração dos tambores foi quase o dobro, quando comparado ao das caixas e baldes. A distribuição dos coeficientes de transferência de calor convectivo ao longo do processo de congelamento não foi constante. Variações e diferentes intensidades de dispersão foram observadas para as diferentes configurações de embalagem e para os diferentes períodos durante o processo de congelamento (pré-resfriamento, mudança de fase e têmpera). A tecnologia de termografia mostrou-se útil no estudo dos coeficientes de transferência de calor, permitindo seu mapeamento completo na superfície da embalagem, sem a necessidade de contato direto com o produto.

Palavras-chave: Coeficiente de transferência de calor convectivo. Câmera de infravermelho. Túnel de congelamento. Consumo energético.

ABSTRACT

The heat transfer process during the freezing of 600 kg of fruit juice model solutions in common containers (boxes, buckets and metallic drums), and different settings in a freezing tunnel, was studied. The air velocity was measured at several points in the entire tunnel. Thermocouples were installed to monitor the temperature profiles within the solution, at the packaging surface and cooling air. To measure the experimental effective heat transfer coefficients conventional temperature measurements with thermocouples and infrared thermography technology were used to map the distribution of the coefficients throughout the surface. Energy consumption involved in each configuration was evaluated. The higher velocities occurred at greater height (above the stacking and drums), being possible to verify the existence of preferential airflow pathways at the opposite ends inside the tunnel. The highest air velocities observed were 2.85 m.s^{-1} ; 2.72 m.s^{-1} and 2.62 m.s^{-1} for drums, boxes and buckets, respectively. The movement of the freezing front has begun from the outermost containers toward those located in the center of the stacks and the average freezing time was 51 h (plastic boxes), 55 h (plastic buckets) and 102 h for metal drums. The energy consumption for drums has been almost the double when comparing with buckets and boxes. The distribution of the local convective heat coefficients throughout the freezing process was not constant. Variations and different intensities of scatter were observed for the different packaging configurations and for the different periods during the freezing process (precooling, phase change and tempering). Thermal imaging technology proved useful in the study of heat transfer coefficients, allowing their complete mapping on the surface of the packaging, without the necessity of direct contact with the product.

Keywords: Convective heat transfer coefficient. Infrared camera. Freezing tunnel. Power consumption.

LISTA DE FIGURAS

PRIMEIRA PARTE

Figura 1 -	Típicas curvas de congelamento para água pura e solução aquosa. Adaptado de Ramaswamy e Tung (1984).....	31
Figura 2 -	Câmeras de imagem térmica.....	39
Figura 3 -	Espectro da radiação eletromagnética.....	40

SEGUNDA PARTE - ARTIGO

Figure 1.	Schematic diagram of the freezing tunnel used in this work and its internal dimensions.	56
Figure 2.	Configuration of the three container settings and the position coordinates of the thermocouples inside. The red dots represent the position of the temperature sensors. (A) - boxes configuration, (B) - buckets configuration and (C) - drums configuration.....	59
Figure 3.	Profiles of the air velocity in the fixed coordinate z - 14 cm (evaporator outlet), and (A) - plastic boxes (B) - plastic buckets and (C) metal drums.	65
Figure 4.	Isotherms obtained during freezing of solution model in plastic boxes and coordinated fixed z = 67.5 cm. (A) - 10 h, (B) - 30 h and (C) - 50 h.	67
Figure 5.	Isotherms obtained during freezing of solution model in buckets and coordinated z = 52 cm (Line 1). (A) - 10 h, (B) - 30 h and (C) - 50 h.....	68
Figure 6.	Isotherms obtained during freezing of solution model in metal drums and coordinated z = 67.5 cm. (A) - 20 h, (B) - 60 h and (C) - 100 h.....	69
Figure 7.	Location of points that demanded more (red) and less time (blue) to reach -18 °C, being (A) - boxes; (B) - buckets and (C) - drums. Freezing time profiles for the boxes (A1), buckets (B1 - line 1 and B2 - line 2) and drums (C1).	71
Figure 8.	Cooling curves of the model solution. SC (supercooling) and T _{if} (initial freezing temperature).	73
Figure 9.	Temperature profiles (solution and air), local convective heat coefficients and their average (before and after freezing the solution). (A) - boxes, (B) - buckets and (C) - drums. (1) - precooling period, (2) - phase change period and (3) - tempering period.	76

Figure 10. Evaluation of the temperature distribution and heat transfer coefficients on the surface for different containers. Boxes (A and B) and buckets (C and D) and drums (E and F). The processing times were: 8.3 h (box), 5.5 h (buckets) e 8.0 h (drums). 81

LISTA DE TABELAS

PRIMEIRA PARTE

Tabela 1 - Teor de sólidos totais mínimo de diferentes polpas de fruta, segundo Brasil (2000).....	27
--	----

SEGUNDA PARTE - ARTIGO

Table 1 - Coefficients of the polynomial equations to evaluate the enthalpy ($\text{kJ} \cdot \text{kg}^{-1}$) in different temperature ranges within the freezing process	74
Table 2 - Average convective coefficients (precooling and tempering period) on the side and top of each studied configuration with the respective standard deviation (SD) and coefficient of variation (CV).....	78
Table 3 - Average processing time, active energy, total area of heat transfer and ratio area per mass during the freezing process of 600 kg of solution, as well as the respective standard deviation (SD) and coefficient of variation (CV).....	83

LISTA DE SÍMBOLOS

<i>a</i>	Coefficient of the equation (5)	-
<i>A</i>	Heat transfer area	m^2
<i>b</i>	Coefficient of the equation (5)	-
<i>Bi</i>	Biot number	-
<i>c</i>	Coefficient of the equation (5)	-
<i>c_p</i>	Specific heat	$\text{kJ} \cdot \text{kg}^{-1} \cdot \text{K}^{-1}$
<i>d</i>	Coefficient of the equation (5)	-
<i>e</i>	Coefficient of the equation (5)	-
<i>h</i>	Convective heat transfer coefficient	$\text{W} \cdot \text{m}^{-2} \cdot {}^\circ\text{C}^{-1}$
<i>H</i>	Enthalpy	$\text{kJ} \cdot \text{kg}^{-1}$
<i>m</i>	Mass	kg
<i>q"</i>	Fluxo térmico por convecção	$\text{W} \cdot \text{m}^{-2}$
<i>T</i>	Temperature	${}^\circ\text{C}$
<i>t</i>	Time	min
<i>x</i>	Depth in the coordinate system	cm
<i>y</i>	Height in the coordinate system	cm
<i>z</i>	Width in the coordinate system	cm

LISTA DE SUBSCRITOS

<i>air</i>	Air
<i>ct</i>	Container
<i>if</i>	Initial freezing
<i>S</i>	Superfície
SC	Subcooling
<i>sol</i>	Solution
∞	Ar de resfriamento

SUMÁRIO

PRIMEIRA PARTE.....	23
1 INTRODUÇÃO	23
2 REFERENCIAL TEÓRICO.....	27
2.1 Polpa de fruta e solução modelo	27
2.2 Congelamento de alimentos.....	29
2.3 Propriedades termofísicas	32
2.3.1 Calor específico	32
2.3.2 Entalpia.....	34
2.3.3 Temperatura de início de congelamento	34
2.4 Velocidade do ar.....	35
2.5 Coeficiente de transferência de calor convectivo	36
2.6 Termografia de infravermelho.....	38
3 CONCLUSÕES	43
REFERÊNCIAS	45
SEGUNDA PARTE - ARTIGO	49
ARTIGO 1 - INFRARED THERMOGRAPHY FOR EVALUATION OF HEAT TRANSFER DURING THE FREEZING OF FRUIT JUICE MODEL SOLUTIONS IN LARGE CONTAINERS.....	49

PRIMEIRA PARTE

1 INTRODUÇÃO

O setor de fruticultura representa um dos mais importantes segmentos da agricultura brasileira, respondendo por grande parcela do valor da produção agrícola nacional e contribui para o desenvolvimento econômico e o crescimento, tanto do mercado de frutas frescas como da sua industrialização, atingindo vários segmentos, como os sucos e as polpas de frutas. A região sul de Minas Gerais tem significativa contribuição nesse setor, sendo produtora de grande variedade de frutíferas que estão disponíveis no mercado, como goiaba, maracujá, pêssego, uva, morango e figo.

Para muitos pequenos produtores, a principal fonte de renda é proveniente do cultivo das frutas, que são sazonais por natureza, o que acaba por gerar altos índices de perdas, dependendo do produto. Este fato motiva e requer o estudo de métodos essenciais que prolonguem o período de armazenamento, os quais podem ser considerados processos-chave de interesse, como o resfriamento e o congelamento. Uma vez implementados dentro de uma prática industrial, eles contribuem para a redução de perdas, tornando os alimentos disponíveis por períodos mais prolongados.

Os túneis de congelamento são largamente utilizados na prática agroindustrial da produção de polpas de frutas, entretanto, o consumo de energia que está relacionado ao tempo de processamento é um fator importante e que pode aumentar o custo global de produção.

Tendo em vista a importância do resfriamento e do congelamento de alimentos e o custo envolvido no processo, um estudo mais detalhado da dinâmica envolvida, com avaliação de propriedades térmicas, simulação e

otimização do processo, bem como o desenvolvimento de novos sistemas e equipamentos, é de grande valia.

Em equipamentos nos quais o escoamento do ar é, geralmente, turbulento e transiente, como nos túneis de congelamento, trocas de calor por convecção são preponderantes. Sendo assim, entre os grandes desafios estão o estudo e a determinação dos coeficientes de transferências de calor convectivo entre a superfície do produto e o ar frio, o que se faz absolutamente necessário para a construção de sistemas de congelamento ou para adaptar condições de operação de sistemas já existentes. Poucos estudos têm sido realizados para medir ou estimar este parâmetro durante o resfriamento e o congelamento de alimentos. Uma das causas mais comuns de erro no cálculo da temperatura dos produtos e do tempo de congelamento origina-se do valor adotado para este coeficiente ou pelo valor obtido aplicando-se algum dos métodos matemáticos conhecidos.

Para auxiliar neste estudo, a técnica de termografia de infravermelho constitui importante ferramenta, possibilitando o monitoramento e a validação de medidas de temperatura, por toda a superfície do produto, as quais são fundamentais para a determinação do coeficiente convectivo de transferência de calor. Diferentemente do método convencional com utilização de termopares, os quais podem alterar o escoamento do ar sobre o produto e por isso dar origem a resultados de medidas de coeficientes não representativos, a termografia faz a aquisição da temperatura de maneira não intrusiva.

Sendo assim, os objetivos do presente trabalho foram: 1) estudar o processo de transferência de calor durante o congelamento de solução modelo de suco de frutas armazenada em diferentes recipientes (caixas, balde e tambores metálicos); 2) determinar, experimentalmente, os coeficientes de transferência de calor convectivos durante todo o processo de congelamento e fazer seu mapeamento sobre a superfície das embalagens com auxílio da tecnologia da

termografia de infravermelho e 3) avaliar o consumo de energia envolvido no processamento, para as três diferentes configurações.

A estrutura deste trabalho se divide em uma primeira parte com um breve referencial teórico e posterior conclusão geral do artigo presente na segunda parte da tese. A segunda parte contém o artigo enviado à revista International Journal of Thermal Sciences, o qual apresenta uma introdução, a especificação da metodologia que foi utilizada para execução do trabalho, todos os resultados e discussões, as conclusões detalhadas, os agradecimentos aos órgãos financiadores e as referências utilizadas.

2 REFERENCIAL TEÓRICO

2.1 Polpa de fruta e solução modelo

Segundo os padrões de identidade e qualidade para polpas de frutas aprovados pela Instrução Normativa nº 01, de 7 de janeiro de 2000 (BRASIL, 2000, p. 54), “polpa de fruta é o produto não fermentado, não concentrado, não diluído, obtido de frutos polposos, através de processo tecnológico adequado, com um teor mínimo de sólidos totais, proveniente da parte comestível do fruto”. A mesma Instrução Normativa estabelece um teor mínimo de sólidos totais para diferentes polpas de fruta, como apresentado na Tabela 1.

Tabela 1 - Teor de sólidos totais mínimo de diferentes polpas de fruta, segundo Brasil (2000).

Polpa	Teor de sólidos totais mínimo (g/100 g)
Acerola	6,5
Cacau	16,0
Cupuaçu	12,0
Graviola	12,0
Açaí	40,0
Maracujá	11,0
Caju	10,5
Manga	14,0
Goiaba	9,0
Pitanga	7,0
Uva	15,0
Mamão	10,5
Cajá	9,5
Melão	7,5
Mangaba	8,5

Na literatura, modelos de predição de propriedades térmicas dos alimentos supõem que os materiais alimentares são soluções binárias ideais, as quais podem ser utilizadas para simular os alimentos em geral (SAAD; SCOTT,

1996). Segundo Resende e Silveira Junior (2002), soluções modelo são extremamente úteis quando se deseja estudar processos ou, ainda, verificar a exatidão de modelos matemáticos de predição.

Modelos para avaliação de propriedades termofísicas dos alimentos presentes na literatura requerem apenas o conhecimento de sua composição centesimal. Eles se baseiam no fato de que os alimentos são constituídos por uma mistura de substâncias puras, tais como carboidratos, proteínas, cinzas, gordura, água e outros componentes e que possuem suas propriedades intrínsecas (AMERICAN SOCIETY OF HEATING - ASHRAE, 2002).

Resende e Silveira Junior (2002) trabalharam com modelo alimentício constituído de 0,5% de K-carrageenan e 10% de sacarose (massa/volume de água), para avaliação das propriedades condutividade e difusividade térmica. Observaram que houve uma importante variação nas propriedades térmicas em baixas temperaturas (0 a -30 °C), devido à alta variação da fração de gelo nesta faixa. Os valores experimentalmente mensurados para condutividade foram comparados com aqueles preditos pelos modelos teóricos em Série, Paralelo e de Maxwell-Eucken, tendo sido neste último em que se obtiveram os menores erros.

Saad e Scott (1996) trabalharam com soluções aquosas de sacarose, metilcelulose e glúten de trigo (4% a 50% em peso) no estudo das propriedades condutividade e calor específico durante seu congelamento. Realizaram medições experimentais e os valores foram comparados com modelos matemáticos. No geral, nas soluções com baixas concentrações de sacarose, os valores experimentais ficaram próximos dos obtidos teoricamente para a condutividade térmica. Entretanto, os dados de calor específico exibiram grandes discrepâncias entre os valores experimentais e teóricos para todas as concentrações de sacarose.

Em ambos os trabalhos citados foi utilizada água como meio dispersor dos sólidos. Isto simula o que ocorre com a maioria dos alimentos que têm um elevado teor de umidade e, consequentemente, a água dispersa os constituintes da mistura alimentar (SAAD; SCOTT, 1996).

2.2 Congelamento de alimentos

O congelamento é uma eficaz forma de preservar os alimentos, o qual é amplamente conhecido e utilizado na indústria. No entanto, considerações matemáticas sobre o processo somente tiveram lugar algumas décadas atrás (DELGADO; SUN, 2001). Para tal procedimento, os túneis de congelamento são os equipamentos mais comumente utilizados. Neles, a temperatura do produto é reduzida pela condução de calor no interior do produto, enquanto a transferência de calor convectiva ocorre entre a sua superfície e o ar de resfriamento (WANG; ZOU, 2014).

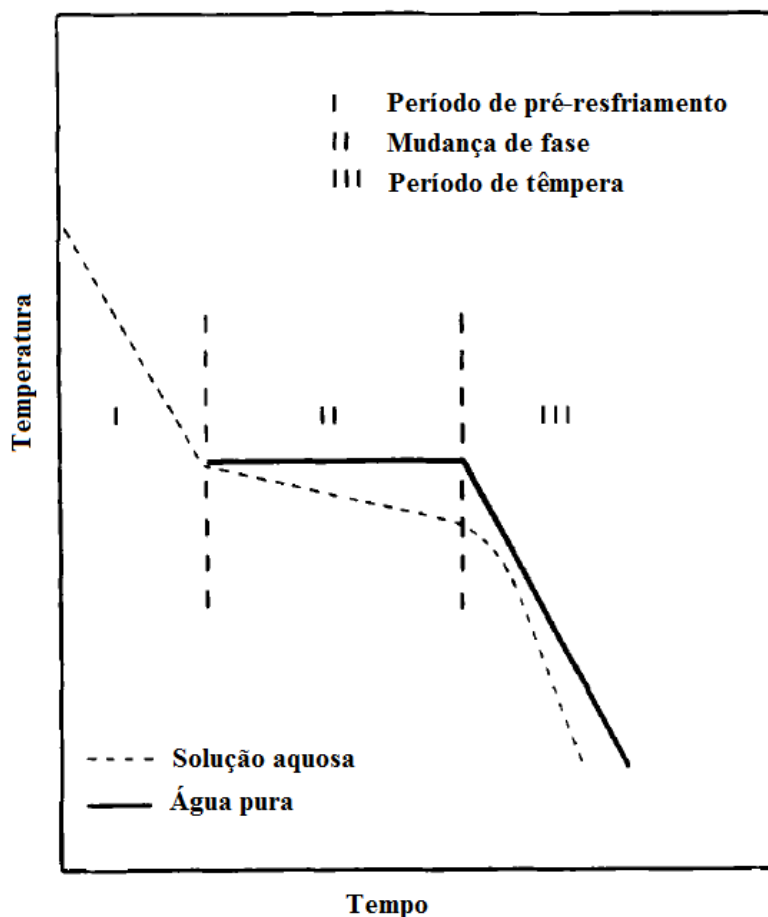
O processo de congelamento combina o efeito favorável de baixas temperaturas com a conversão de água em gelo. Em temperaturas de congelamento inferiores a -10 °C, poucos microrganismos podem se desenvolver, as taxas de reação química são muito reduzidas e as reações metabólicas celulares também são atrasadas (DELGADO; SUN, 2001).

Para o armazenamento de alimentos congelados, a temperatura recomendada é de -18 °C. Temperaturas inferiores a essa podem ser utilizadas, porém, elevam bastante o custo de manutenção do produto. Uma vez congelados, flutuações na temperatura devem ser, ao máximo, evitadas, uma vez que poderão provocar recristalizações, as quais podem gerar aumento do tamanho dos cristais de gelo, o que é altamente prejudicial para a textura de muitos produtos congelados (PARDI et al., 2001).

Para frutas na sua forma de polpa, o efeito do processo de congelamento é verificado pela alteração na consistência da polpa e por meio de mudanças em sua composição, causadas por reações químicas que ocorrem durante o armazenamento posterior. A sua consistência e a aparência global são mais bem mantidas quando o processo é feito em alta velocidade (WANG; CHANG, 1994).

Segundo Ramaswamy e Tung (1984), o processo de congelamento pode ser dividido em três fases distintas: um período de pré-resfriamento, no qual o material é resfriado desde a sua temperatura inicial até ao ponto de início de congelamento; um período de mudança de fase, em que todo o calor latente é liberado e um período de têmpera, em que a temperatura é reduzida para a temperatura alvo, como apresentado na Figura 1.

Figura 1 - Típicas curvas de congelamento para água pura e solução aquosa.
Adaptado de Ramaswamy e Tung (1984).



No período de pré-resfriamento, os fatores que contribuem para a carga de calor são as propriedades térmicas dos materiais não congelados e a diferença de temperatura inicial e de início de congelamento do produto. O período de mudança de fase caracteriza-se pela cristalização da água em gelo, o que ocorre pela nucleação e o aumento dos cristais. O período de têmpera é governado pelas propriedades do material já congelado e pela diferença entre a temperatura de início de congelamento e a temperatura alvo. Além disso, devido à presença de

sólidos dissolvidos e à interação de outros constituintes dos alimentos com quantidades relativamente grandes de água contida no material alimentar, o ponto de congelamento sofre uma depressão abaixo do ponto de início de congelamento da água pura, sendo a magnitude da depressão dependente da natureza do alimento.

2.3 Propriedades termofísicas

O conhecimento das propriedades termofísicas dos alimentos é essencial para o estudo e os cálculos de transferência de calor que estão envolvidos em projetos de equipamentos de refrigeração e armazenamento de alimentos (ASHRAE, 2002). São importantes, pois influenciam a capacidade de um sistema de refrigeração, bem como a velocidade do congelamento (RESENDE; SILVEIRA JUNIOR, 2002). Os dados das propriedades podem ser utilizados para avaliação do coeficiente de transferência de calor convectivo, na simulação da temperatura dos alimentos durante o congelamento e armazenamento, sendo também importantes para a estimativa do tempo de congelamento. A simulação do processo de congelamento é de grande importância para a concepção de técnicas de congelamento superior e equipamentos de refrigeração mais eficientes (SAAD; SCOTT, 1996).

Importantes propriedades térmicas e que foram essenciais neste trabalho para avaliação do coeficiente de transferência de calor convectivo são calor específico, entalpia e temperatura de início de congelamento.

2.3.1 Calor específico

Calor específico é uma medida da energia necessária para mudar a temperatura de um alimento em um grau, em uma unidade de massa, sem

mudança de estado. Portanto, o calor específico de alimentos pode ser utilizado para calcular a carga térmica imposta aos equipamentos de refrigeração por resfriamento ou congelamento (ASHRAE, 2002). Nos processos de transferência de calor a que são submetidos os materiais biológicos, a variação de pressão é muito pequena. Portanto, utiliza-se o conceito de calor específico a pressão constante (MOHSENNIN, 1980).

Dentre os métodos utilizados para a medição do calor específico, a metodologia de calorimetria diferencial de varredura (DSC) é altamente utilizada (RAHMAN, 2009). É uma técnica termoanalítica baseada na medição de pequenos efeitos produzidos em processos térmicos (MOHSENNIN, 1980). As vantagens de se utilizar o DSC são a rapidez de medidas, a obtenção de dados múltiplos em um único termograma e o uso de uma pequena quantidade de amostras, gerando resultados precisos (MURPHY; MARKS; MARCY, 1998).

No método do DSC, a quantidade de energia necessária para variar a temperatura da amostra é comparada com a energia necessária para mudar a temperatura de um material de referência, sob a mesma taxa de aquecimento. O calor requerido para atingir a temperatura é gravado em um termograma, que registra o histórico do fluxo de calor relacionado com a temperatura (MATTOS, 2007). Os termogramas mostram qualquer ganho ou perda de energia térmica referente a um aumento de temperatura em um dado intervalo de temperatura. A natureza dinâmica do processo permite a determinação do calor específico em função da temperatura (SINGH; GOSWAMI, 2000) e os fatores que podem afetar os valores medidos para o calor específico podem ser o tamanho da amostra, a taxa de aquecimento e as condições de vedação da amostra (RAHMAN, 2009).

Zainal et al. (2000) avaliaram, com metodologia de DSC, o efeito da temperatura sobre o calor específico de suco de goiaba vermelha em duas concentrações diferentes (9° Brix e 11° Brix). Tansakul et al. (2012) utilizaram a

calorimetria diferencial de varredura para a determinação do calor específico de purê de mamão, em relação ao teor de sólidos solúveis e da temperatura.

2.3.2 Entalpia

A entalpia de um alimento é uma propriedade que pode ser utilizada para estimar a energia que deve ser adicionada ou removida para efetuar uma mudança de temperatura. Acima da temperatura inicial de congelamento a entalpia consiste em energia sensível; já abaixo do ponto de congelamento, consiste em energia sensível e latente. A entalpia pode ser obtida a partir da definição de calor específico de pressão constante (ASHRAE, 2002).

$$c_p = \left(\frac{\partial H}{\partial T} \right)_p \quad (1)$$

em que

c_p - calor específico a pressão constante ($\text{kJ} \cdot \text{kg}^{-1} \cdot \text{K}^{-1}$),

H - entalpia ($\text{kJ} \cdot \text{kg}^{-1}$),

T - temperatura ($^{\circ}\text{C}$).

2.3.3 Temperatura de início de congelamento

A temperatura inicial de congelamento é aquela em que os cristais de gelo aparecem pela primeira vez em um ponto onde ambas as fases, líquido (água) e sólido (cristal de gelo), coexistem em equilíbrio. Os cristais se separam da solução e provocam a concentração cada vez maior do soluto na solução remanescente. Sendo os alimentos sistemas de multicomponentes, em que há minerais e compostos orgânicos, incluindo ácidos, gorduras, gases, proteínas,

sais e açúcares dispersos em água, que é o principal componente, a temperatura em que o fenômeno de formação dos cristais começa a acontecer é ligeiramente inferior ao ponto de congelamento da água pura e é definida como a temperatura de início de congelamento do alimento (RAHMAN, 2009). Segundo Carson (2006), para alimentos com alto teor de umidade, como frutas frescas, legumes, carne e produtos do mar, a temperatura de início de congelamento está, normalmente, na faixa entre -0,5 °C a -3,0 °C.

De acordo com Rahman (2009), um método amplamente utilizado para a determinação da temperatura de início de congelamento é a curva de resfriamento, por meio da aquisição de dados experimentais de temperatura em função do tempo durante o congelamento, sendo um método bastante simples e preciso.

2.4 Velocidade do ar

Na indústria de alimentos, a utilização do ar frio é uma maneira comum de refrigeração e congelamento (ALONSO et al., 2011) e este é o meio de resfriamento dos túneis de congelamento com corrente forçada. Nestas situações, a distribuição espacial da velocidade do ar sobre os empilhamentos e o consumo de energia para movê-lo e passá-lo pelo produto são as duas principais considerações a serem feitas (EARLE, 1985). A distribuição do fluxo de ar afeta, ainda, a homogeneidade e o tempo de congelamento, os quais são dois critérios economicamente importantes de eficiência do processo (ALONSO et al., 2011). Um campo uniforme de velocidade proporciona tempos de congelamento homogêneos para os produtos, mas é complicado de se conseguir (WIDELL, 2011).

A preocupação envolvida na distribuição do ar em relação à geometria da câmara e à uniformidade da trajetória do escoamento nos processos de

resfriamento e congelamento rápidos vem do fato de que, na grande parte das instalações, o ar sofre grande variabilidade na sua velocidade no espaço e no tempo, tornando seu controle um ponto crítico (RESENDE; NEVES FILHO; SILVEIRA JUNIOR, 2002). Segundo Mirade e Daudin (1998), as dificuldades relacionadas às medidas são devido à alta instabilidade e ao fato de que a direção do escoamento é fortemente influenciada pela presença de objetos, o que gera turbulência.

Resende, Neves Filho e Silveira Junior (2002) afirmam que os resultados mensurados para velocidade do ar, que são utilizados para a determinação da vazão e cálculos de transferência de calor, muitas vezes, podem não ser muito confiáveis, o que traz incertezas sobre os coeficientes de transferência de calor superficiais obtidos no processo.

2.5 Coeficiente de transferência de calor convectivo

Muitos dos processos industriais baseiam-se em uma transferência simultânea de calor e massa entre um sólido e um fluido, sendo frequentemente aplicados no processamento de alimentos, tais como na refrigeração e no congelamento rápidos. Logo que a velocidade do ar se torna superior a $0,4/0,5 \text{ m.s}^{-1}$, trocas de calor por convecção se tornam predominantes dentro do sistema. Sendo assim, a determinação do fluxo de calor do fluido de resfriamento para a superfície do produto pode ser calculada se os valores dos coeficientes de transferência de calor convectivos são conhecidos (GHISALBERTI; KONDJOYAN, 2001).

Basicamente, a transferência de calor por convecção é regida pela Lei do Resfriamento de Newton, como apresentado na equação 2 (BERMGAN et al., 2014).

$$q'' = h(T_s - T_\infty) \quad (2)$$

em que

q'' - fluxo térmico por convecção ($\text{W} \cdot \text{m}^{-2}$);

h - coeficiente de transferência de calor por convecção ($\text{W} \cdot \text{m}^{-2} \cdot ^\circ\text{C}^{-1}$);

T_s - temperatura da superfície ($^\circ\text{C}$);

T_∞ - temperatura do ar de resfriamento ($^\circ\text{C}$).

A importância do conhecimento da distribuição do coeficiente de transferência de calor nos processos industriais de resfriamento e congelamento está no fato de que eles governam a taxa de resfriamento que está relacionada ao tempo de residência do produto no equipamento e, consequentemente, ao consumo de energia. No âmbito de qualidade do produto, seu conhecimento poderá ser utilizado para predizer riscos de danos e deterioração nas superfícies do produto devido a tratamentos intensivos de resfriamento (GHISALBERTI; KONDJOYAN, 2001).

Segundo Amarante e Lanoiselé (2005), o coeficiente de transferência de calor convectivo é um parâmetro, muitas vezes, complexo de ser estimado, sendo um grande desafio sua avaliação, principalmente em processos turbulentos, como dentro de um túnel de congelamento, devido ao fato de a taxa de transferência de calor ser altamente dependente das condições de escoamento do ar. Nestes processos, variações locais nos coeficientes são esperadas ao longo da superfície, resultando também em diferenças locais nas temperaturas (PHAM; TRUJILLO; MCPHAIL, 2009). Sendo assim, pode-se dizer que o perfil de velocidade do ar determina a eficiência e a homogeneidade dos tratamentos de resfriamento e congelamento de alimentos.

Uma das causas mais comuns de erro no cálculo da temperatura dos produtos origina-se do valor adotado para este coeficiente, ou pelo valor obtido

aplicando-se algum dos métodos matemáticos conhecidos (RESENDE; NEVES FILHO; SILVEIRA JUNIOR, 2002). Utilizando-se métodos experimentais, a sua determinação é complexa, pela quantidade de fatores que a influenciam. Um deles é a própria aquisição das medidas da temperatura nas superfícies das amostras, havendo dificuldade de colocação e fixação de sensores nas superfícies, os quais podem alterar as propriedades do escoamento do ar sobre a mesma, implicando em um grau de incerteza grande nos coeficientes obtidos (GHISALBERTI; KONDJOYAN, 2001). Quando a forma da amostra é elementar, poucos termopares são necessários para as medidas, mas, para formatos mais complexos, o número de termopares tem de ser aumentado para descrever adequadamente a distribuição do coeficiente de transferência de calor. Para superar esta dificuldade, a temperatura da superfície pode ser medida utilizando-se câmeras de infravermelho. Contudo, esta técnica ainda tem sido pouco empregada para determinar os coeficientes de transferência de calor, principalmente em processos em baixas temperaturas (GHISALBERTI; KONDJOYAN, 2001).

2.6 Termografia de infravermelho

Nos últimos anos, têm-se investigado cada vez mais novas tecnologias para monitorar a qualidade e a segurança de alimentos. Uma delas é a termografia de infravermelho, que é uma técnica diagnóstica bidimensional, utilizada para medir a temperatura superficial dos materiais e que pode ser utilmente empregada na avaliação da qualidade (GOWEN et al., 2010). Esta técnica de processamento de imagem transforma a radiação térmica em um termograma, que é uma imagem visual detalhada em um perfil de temperaturas (VERAVERBEKE et al., 2006). Para tal, é utilizado um equipamento chamado

termovisor (Figura 2), o qual é, basicamente, uma câmera que detecta a energia eletromagnética irradiada na banda espectral do infravermelho (IR).

Figura 2 - Câmeras de imagem térmica.

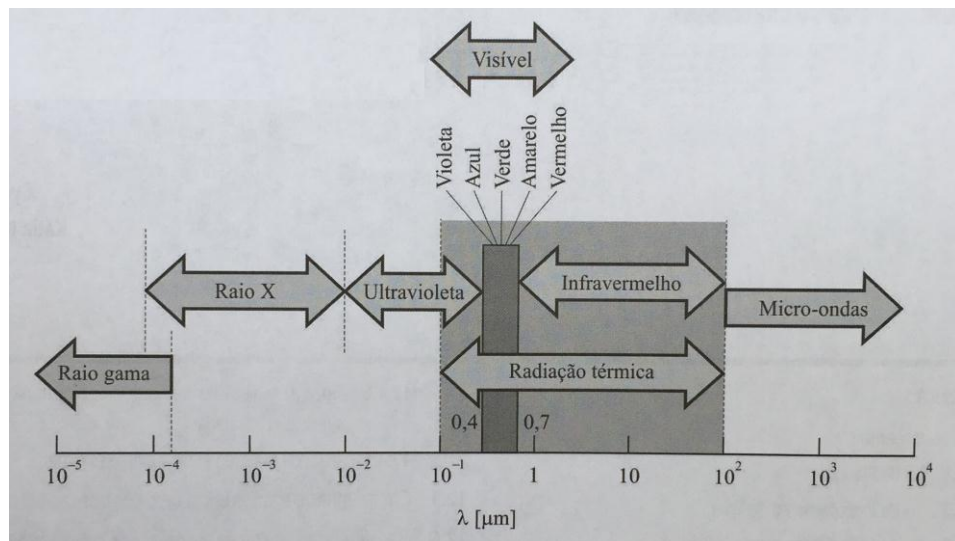


Fonte: FLIR Systems (2016)

O princípio básico da imagem térmica é baseado no fato de que todo objeto, estando em temperaturas acima do zero absoluto, emite radiação infravermelha. O termovisor capta esta radiação e a converte em um sinal elétrico, dando origem a uma matriz de dados que será posteriormente transformada na imagem termográfica. O detector é o núcleo do sistema de termografia de infravermelho (CARLOMAGNO; DE LUCA, 1991).

O espectro eletromagnético completo está apresentado na Figura 3. Neste espectro, a radiação térmica representa uma fração da radiação ultravioleta, todo o visível e o infravermelho, a qual abrange o comprimento de onda entre 0,1 a 100 μm . É nesta faixa que o estado térmico, ou temperatura da matéria, é afetado (BERMGAN et al., 2014).

Figura 3 - Espectro da radiação eletromagnética.



Fonte: Bergman et al. (2014).

A vantagem potencial do uso da termografia na análise do processo de transferência de calor, comparada aos métodos convencionais com termômetros, termopares e termorresistências, é que ela é capaz de quantificar as mudanças na temperatura da superfície com resolução temporal e espacial elevada, enquanto os métodos convencionais proporcionam medições de ponto único. As avaliações de fluxo térmico com os métodos convencionais pontuais são limitadas, o que torna um problema sempre que os campos de temperatura exibem variações espaciais elevadas. Em vez disso, a câmara infravermelha constitui um transdutor bidimensional, permitindo medições precisas de mapas de temperatura superficial, mesmo na presença de gradientes espaciais relativamente grandes (CARLOMAGNO; CARDONE, 2010). A termografia é, ainda, uma técnica de avaliação muito rápida, que permite a medição de objetos em movimento. É uma técnica não destrutiva e na qual não há necessidade de contato, o que não interfere, por exemplo, nas características de um escoamento

e garante prevenção de contaminação do alimento por contato (GOWEN et al., 2010; IBARRA et al., 1999).

Especificamente na avaliação do coeficiente de transferência de calor por convecção, o uso de métodos termográficos permite uma interpretação baseada nas suas variações locais. Reduz, assim, o número de experimentos que seriam necessários para explicar mecanismos que dependem de muitos fatores, tais como velocidade e turbulência do escoamento, forma e dimensões do produto (GHISALBERTI; KONDJOYAN, 2001).

Fito et al. (2004) empregaram imagens térmicas para modelar a cinética de desidratação de frutas cítricas durante a secagem, por meio de medidas da distribuição de temperatura. Elas puderam ser utilizadas para determinar o ponto de secagem final e também desenvolver sistemas de controle *on-line*.

Björk, Björn e Nordenberg (2010) utilizaram uma câmera termográfica para observar a distribuição de temperatura em um sistema de refrigeração de um refrigerador doméstico operando em ciclos liga-desliga. As análises permitiram visualizar como a carga de refrigerante é distribuída através do sistema de resfriamento em condições transientes. Também foi possível identificar as perdas de energia em pontos do sistema que seriam difíceis de serem localizadas com medidas usando termopares convencionais.

Gonçalves et al. (2016) utilizaram a termografia durante o resfriamento e o armazenamento de goiabas a diferentes temperaturas, no intuito de identificar danos causados no tecido. Injúrias mecânicas, causadas pelo impacto de um pêndulo, foram induzidas nas superfícies de goiabas e, com a termografia, foi possível distinguir os tecidos lesados dos frutos que não foram afetados a temperaturas de 5 °C, 10 °C e 20 °C.

Reno et al. (2011) avaliaram o processo de transferência de calor, incluindo coeficientes convectivos, tempos de congelamento e consumo de energia em túneis de congelamento de baixo custo utilizados para o

congelamento de polpas de goiaba em diferentes embalagens. Os resultados mostraram que, em todas as configurações, os recipientes localizados mais próximos da porta foram os últimos a congelar. Utilizando uma câmera de infravermelho foram obtidos termogramas que mostraram a existência e a influência de fontes de calor externo por infiltração, provenientes do ambiente externo, que justificaram os perfis de temperatura.

3 CONCLUSÕES

No trabalho apresentado na segunda parte desta tese, o artigo enviado à revista International Journal of Thermal Sciences, foi possível estudar a dinâmica do processo de transferência de calor durante o congelamento de soluções modelo de suco de frutas em um túnel de congelamento com ar forçado. Com as diferentes embalagens e configurações comerciais estudadas, foi possível avaliar a distribuição das temperaturas da solução, dos recipientes e do ar de resfriamento, bem como avaliar os perfis de velocidade formados dentro do túnel. Além disso, com um balanço de energia aplicado ao sistema podem-se determinar os coeficientes de transferência de calor convectivos durante todo o processo de congelamento.

O principal resultado do trabalho foi o próprio método experimental. A metodologia proposta de termografia de infravermelho mostrou-se útil no estudo dos coeficientes de transferência de calor convectivos, permitindo seu mapeamento por toda a superfície da embalagem, sem a necessidade de contato direto com o produto. Seu uso pode ser uma técnica alternativa e com vantagens significativas sobre o procedimento tradicional com o uso de termopares para avaliar os processos térmicos dentro das práticas da indústria de alimentos.

REFERÊNCIAS

- ALONSO, M. J. et al. Improvements of air flow distribution in a freezing tunnel using Airpak. **Procedia Food Science**, Amsterdam, v. 1, p. 1231-1238, 2011.
- AMARANTE, A.; LANOISELLÉ, J. L. Heat transfer coefficients measurement in industrial freezing equipment by using heat flux sensors. **Journal of Food Engineering**, Essex, v. 6, p. 377-386, Feb. 2005.
- AMERICAN SOCIETY OF HEATING. **ASHRAE handbook:** refrigeration. Atlanta: Refrigeration and Air-conditioning Engineers, 2002.
- BERGMAN, T. L. et al. **Fundamentos de transferência de calor e de massa**. Rio de Janeiro: LTC, 2014. 672 p.
- BJÖRK, E.; BJÖRN, P.; NORDENBERG, J. A thermographic study of the on-off behavior of an all-refrigerator. **Applied Thermal Engineering**, Oxford, v. 30, p. 1974-1984, Oct. 2010.
- BRASIL. Instrução Normativa nº 01, de 7 de janeiro de 2000. Regulamento técnico geral para fixação dos padrões de identidade e qualidade para polpa de fruta. **Diário Oficial da União**, Brasília, DF, 10 jan. 2000. Seção 1, p. 54-55.
- CARLOMAGNO, G. M.; CARDONE, G. Infrared thermography for convective heat transfer measurements. **Experiments in Fluids**, Berlin, v. 49, p. 1187-1218, Dec. 2010.
- CARLOMAGNO, G. M.; DE LUCA, L. Infrared thermography for flow visualization and heat transfer measurements. In: ATTI WORSHOP (STATO DELL'ARTE DEL RILEVAMENTO CON CAMERE TERMICHE NELLA BANDA 8-14 MICRON), 1991, Firenze. **Proceedings...** Firenze, 1991. p. 191-219.
- CARSON, J. K. Review of effective thermal conductivity models for food. **International Journal of Refrigeration**, Surrey, v. 29, n. 6, p. 958-967, July 2006.
- DELGADO, A. E.; SUN, D. W. Heat and mass transfer models for predicting freezing processes: a review. **Journal of Food Engineering**, Essex, v. 47, p. 157-174, Feb. 2001.

EARLE, R. L. Freezing of foods: an overview food engineering and process applications. **Food Engineering and Process Applications**, Alberta, v. 2, p. 3-20, 1985.

FITO, P. J. et al. Control of citrus surfaces drying by image analysis of infrared thermography. **Journal of Food Engineering**, Essex, v. 61, p. 287-290, Feb. 2004.

FLIR SYSTEMS. Disponível em: <<http://www.flir.com.br>>. Acesso em: 10 out. 2016.

GONÇALVES, B. J. et al. Using infrared thermography to evaluate the injuries of cold-stored guava. **Journal of Food Science and Technology**, Trivandrum, v. 53, p. 1063-1070, Feb. 2016.

GOWEN, A. A. et al. Applications of thermal imaging in food quality and safety assessment. **Trends in Food Science & Technology**, Cambridge, v. 21, p. 190-200, Apr. 2010.

GHISALBERTI, L.; KONDJOYAN, A. A thermographic method to map the local heat transfer coefficient on the complete surface of a circular cylinder in an airflow. **International Journal of Thermal Science**, New York, v. 40, p. 738-752, Sept. 2001.

IBARRA, J. G. et al. Internal temperature of cooked chicken meat through infrared imaging and time series analysis. **Transactions of ASAE**, Saint Joseph, v. 42, p. 1383-1390, 1999.

MATTOS, J. S. **Banco de dados de propriedades termofísicas de produtos hortícolas**. 2007. 128 f. Dissertação (Mestrado em Engenharia Agrícola)-Universidade Estadual de Campinas, Campinas, 2007.

MIRADE, P. S.; DAUDIN, J. D. A new experimental methods for visualizing air flow in large food plants. **Journal of Food Engineering**, Essex, v. 36, p. 31-49, Apr. 1998.

MOHSENNIN, N. N. **Thermal properties of foods and agricultural materials**. London: Gordon and Breach, 1980. 408 p.

MURPHY, R. Y.; MARKS, B. P.; MARCY, J. A. Apparent specific heat of chicken breast patties and their constituent proteins by differential scanning calorimetry. **Journal of Food Science**, Chicago, v. 63, n. 1, p. 88-91, Mar. 1998.

PARDI, M. C. et al. Ciência e higiene da carne: tecnologia da sua obtenção e transformação. In: _____. **Ciência, higiene e tecnologia da carne**. 2. ed. Goiânia: Ed. UFG, 2001. v. 1, p. 560-571.

PHAM, Q. T.; TRUJILLO, F. J.; MCPHAIL, N. Finite element model for beef chilling using CFD: generated heat transfer coefficients. **International Journal of Refrigeration**, Surrey, v. 32, p. 102-113, Jan. 2009.

RAHMAN, M. S. **Food properties handbook**. 2nd ed. Boca Raton: CRC, 2009. 859 p.

RAMASWAMY, H. S.; TUNG, M. A. A review on predicting freezing times of foods. **Journal of Food Process Engineering**, Westport, v. 7, p. 169-203, July 1984.

RENO, M. J. et al. Heat transfer and energy consumption in the freezing of guava pulp in large containers. **Applied Thermal Engineering**, Oxford, v. 31, p. 545-555, Mar. 2011.

RESENDE, J. V.; NEVES FILHO, L. C.; SILVEIRA JUNIOR, V. Escoamento de ar através de embalagens de polpa de frutas em caixas comerciais: efeitos sobre os perfis de velocidade em túneis de congelamento. **Ciência e Tecnologia de Alimentos**, Campinas, v. 22, p. 184-191, maio/ago. 2002.

RESENDE, J. V.; SILVEIRA JUNIOR, V. Medidas da condutividade térmica efetiva de modelos de polpas de frutas no estado congelado. **Ciência e Tecnologia de Alimentos**, Campinas, v. 22, p. 177-183, maio/ago. 2002.

SAAD, Z.; SCOTT, E. P. Estimation of temperature dependent thermal properties of basic food solutions during freezing. **Journal of Food Engineering**, Essex, v. 28, p. 1-19, Apr. 1996.

SINGH, K. K.; GOSWAMI, T. K. Thermal properties of cumin seed. **Journal of Food Engineering**, Essex, v. 45, n. 4, p. 181-187, Sept. 2000.

TANSAKUL, A. et al. Thermophysical properties of papaya puree. **International Journal of Food Properties**, Philadelphia, v. 15, n. 5, p. 1086-1100, 2012.

VERAVERBEKE, E. A. et al. Thermographic surface quality evaluation of apple. **Journal of food engineering**, Essex, v. 77, p. 162-168, Nov. 2006.

WANG, C. C. H.; CHANG, K. C. Beet pulp and isolated pectin physicochemical properties as related to freezing. **Journal of Food Science**, Oxford, v. 59, p. 113-1154, Nov. 1994.

WANG, G.; ZOU, P. Mathematical modeling of food freezing in air-blast freezer. **International Journal of Materials, Mechanics and Manufacturing**, Singapore, v. 2, p. 278-281, Nov. 2014.

WIDELL, K. N. **Energy efficiency of freezing tunnels:** towards an optimal operation of compressors and air fans. 2011. 101 p. Thesis (Ph.D. in Philosophiae)-Norwegian University of Science and Technology, Trondheim, 2011.

ZAINAL, B. S. et al. Effects of temperature on the physical properties of pink guava juice at two different concentrations. **Journal of Food Engineering**, Essex, v. 43, n. 1, p. 55-59, Jan. 2000.

SEGUNDA PARTE - ARTIGO

ARTIGO 1

INFRARED THERMOGRAPHY FOR EVALUATION OF HEAT TRANSFER DURING THE FREEZING OF FRUIT JUICE MODEL SOLUTIONS IN LARGE CONTAINERS

Cristina Guimarães Pereira^{a*}, Hosahalli S. Ramaswamy^{b*}, Tales Márcio de Oliveira Giarola^a and Jaime Vilela de Resende^{a*}

^aDepartment of Food Science, Laboratory of Food Refrigeration, Federal University of Lavras, P.O. Box 3037, 37200-000, Lavras, Minas Gerais, Brazil

^bDepartment of Food Science and Agricultural Chemistry, Macdonald Campus, McGill University, 21111 Lakeshore Road, Ste. Anne de Bellevue, Québec, H9X 3V9, Canada

*Corresponding authors. Tel.: +55 35 38291050; +1 514 398 7919;

fax: +1 514 398 7977

E-mail addresses: crisgp13@yahoo.com.br (C.G. Pereira);

hosahalli.ramaswamy@mcgill.ca (H.S. Ramaswamy); jvresende@dca.ufla.br
(J.V. Resende)

**Artigo preparado de acordo com as normas da revista *International Journal
of Thermal Sciences***

Abstract

The heat transfer process during the freezing of 600 kg of fruit juice model solutions in common containers (boxes, buckets and metallic drums), and different settings in a freezing tunnel, was studied. The air velocity was measured at several points in the entire tunnel. Thermocouples were installed to monitor the temperature profiles within the solution, at the packaging surface and cooling air. To measure the experimental effective heat transfer coefficients conventional temperature measurements with thermocouples and infrared thermography technology were used to map the distribution of the coefficients throughout the surface. Energy consumption involved in each configuration was evaluated. The higher velocities occurred at greater height (above the stacking and drums), being possible to verify the existence of preferential airflow pathways at the opposite ends inside the tunnel. The highest air velocities observed were 2.85 m.s^{-1} ; 2.72 m.s^{-1} and 2.62 m.s^{-1} for drums, boxes and buckets, respectively. The movement of the freezing front has begun from the outermost containers toward those located in the center of the stacks and the average freezing time was 51 h (plastic boxes), 55 h (plastic buckets) and 102 h for metal drums. The energy consumption for drums has been almost the double when comparing with buckets and boxes. The distribution of the local convective heat coefficients throughout the freezing process was not constant. Variations and different intensities of scatter were observed for the different packaging configurations and for the different periods during the freezing process (precooling, phase change and tempering). Thermal imaging technology proved useful in the study of heat transfer coefficients, allowing their complete mapping on the surface of the packaging, without the necessity of direct contact with the product.

Keywords: convective heat transfer coefficient; infrared camera; freezing tunnel; power consumption.

Nomenclature

<i>a</i>	Coefficient of the equation (5)	-
<i>A</i>	Heat transfer area	m^2
<i>b</i>	Coefficient of the equation (5)	-
<i>Bi</i>	Biot number	-
<i>c</i>	Coefficient of the equation (5)	-
<i>c_p</i>	Specific heat	$\text{kJ} \cdot \text{kg}^{-1} \cdot \text{K}^{-1}$
<i>d</i>	Coefficient of the equation (5)	-
<i>DSC</i>	Differential scanning calorimeter	-
<i>e</i>	Coefficient of the equation (5)	-
<i>h</i>	Convective heat transfer coefficient	$\text{W} \cdot \text{m}^{-2} \cdot \text{K}^{-1}$
<i>H</i>	Enthalpy	$\text{kJ} \cdot \text{kg}^{-1}$
<i>m</i>	Mass	kg
<i>T</i>	Temperature	$^{\circ}\text{C}$
<i>t</i>	Time	min
<i>x</i>	Depth in the coordinate system	cm
<i>y</i>	Height in the coordinate system	cm
<i>z</i>	Width in the coordinate system	cm

Subscripts

<i>air</i>	Air
<i>ct</i>	Container
<i>if</i>	Initial freezing
<i>p</i>	Pressure
SC	Subcooling
<i>sol</i>	Solution

1. Introduction

Many industrial processes are based on a simultaneous heat and mass transfer between a solid of complex shape and an air flow. This is what normally occurs in food processing when applying techniques such as refrigeration, freezing and drying [1]. These processes are considered to be of great interest to add value to food, because once implemented in an industrial practice, they contribute to the reduction of losses, making them available for longer periods.

A large increase in the production and consumption of fruit pulp, juice and other fruit products has been recorded over the last decade [2], which generates an increasing interest in determining thermal properties, simulation and optimization of processes, as well the development of new systems and equipments in this area. In a freezing system, the simulation of its performance is required for its design, adaptation and operation. For this, the accurate knowledge of the heat transfer coefficients is essential in order to obtain a reliable prediction. However, this parameter is often complex to be estimated in industrial processing conditions such as a freezing tunnel [3].

Researchers have noted that the velocity of fluid through the product is the most significant factor influencing the surface heat transfer coefficient [4] and the air flow is a critical point in the installation. Due its strong variability in space and time, its measurement is considered a challenge, which often produces unreliable results that are subsequently used in the heat transfer calculations, such as the determination of the heat transfer coefficients [5,3]. Uncertainty in the order of 10 to 30% is commonly reported in the literature for this parameter [6,7].

Temperature acquisition at the surface of the sample are needed to determine the local heat transfer coefficients. However, the measurements using conventional experimental methods such as thermometers and thermocouples is

done with relative difficulty due the placement and attachment of sensors. The problem is in the fact that they can change the flow properties on the product surface, because when its form is elementary, just few thermocouples are needed for the measures, but when there are more complex shapes, the number of thermocouples must be increased to adequately describe the distribution of the heat transfer coefficient [1].

Within this context new and innovative technologies have been invested to assist the processes occurring in food industry in order to increase their quality and safety. Among them we can mention the infrared thermography (IR), a powerful experimental tool for non-intrusive measurements of temperature in areas of particular interest in industrial applications such as inspection and quality control, but also in scientific applications such as the local identification of thermophysical parameters [8,9]. The potential advantages of their use in processes involving heat transfer compared to tests of invasive sampling with thermocouples and conventional thermometers include high-speed, non-intrusive analysis that do not interfere at the flow characteristics and do not bring interference due the heat conduction through the thermocouple, still avoid contamination by contact with the product [8,9,10]. Moreover, as a two-dimensional measurement technology, the IR camera is able to produce a full field of view on the surface of a product, effectively making it possible to measure convective heat flows [8,9].

Since information on heat transfer coefficients in industrial scale equipment is scarce in the literature [3], the objective of this work was: 1) to study the heat transfer process during the freezing of fruit juice model solution in common containers (boxes, buckets and metallic drums), and different settings in a freezing tunnel; 2) to measure the experimental effective heat transfer coefficients in these configurations using conventional temperature measurements with thermocouples and infrared thermography technology to

map the distribution of the coefficients on the surfaces of packaging, and 3) to evaluate the energy consumption involved in the processing for the three configurations considering a fixed quantity of the product.

2. Material and methods

2.1. Freezing of solution model

A model solution was used to simulate fruit juices, which consisted of 0.5% of k-carrageenan (weight/volume in water) and 10% sucrose (weight/volume in water). The k-carrageenan was added in order to avoid convection processes within the solution and the sucrose used could simulate fruit juice/pulp. The cooling and freezing of the solution were carried out in an air blast freezer under controlled condition at -25 °C. The load consisted of 3 packing configurations: either 40 of high density polyethylene buckets (HDPE) with 15 kg of solution, 40 HDPE boxes of 15 kg of solution each or three metal drums with 200 kg of solution each, totaling 600 kg in each case. For the boxes and drums, plastic bags of polyethylene were used for holding the solution. Fig. 1 shows the internal dimensions of the freezing tunnel, the direction of air flow, the positioning of the inspection windows and the rectangular coordinate system (x, y, z) which was used as a reference in all configurations throughout this work. The coordinates x, y and z represent the dimensions of depth, height and width, respectively.

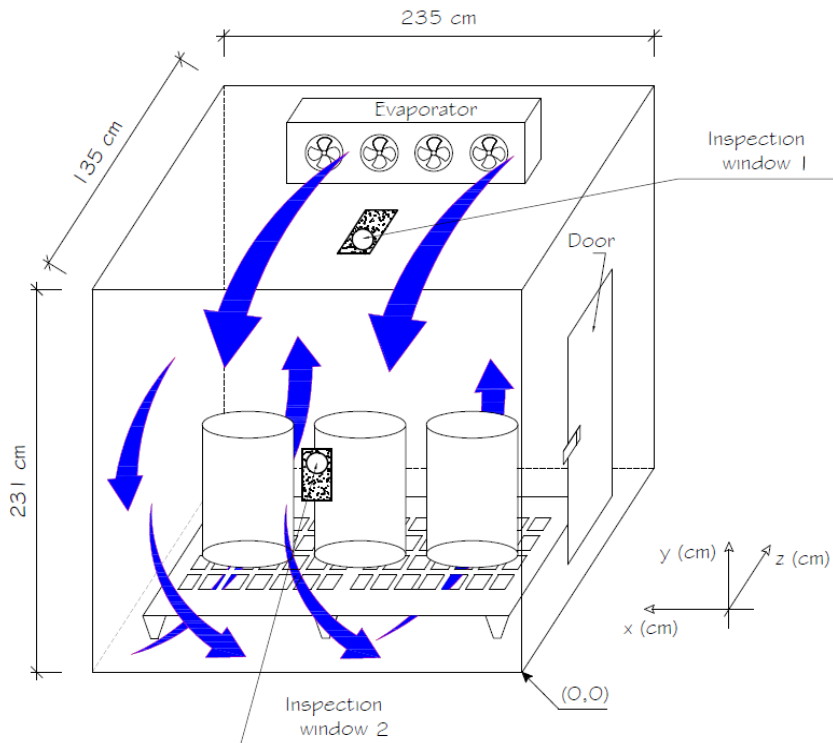


Figure 1. Schematic diagram of the freezing tunnel used in this work and its internal dimensions.

The positioning of inspection windows were set in (x, y and z) coordinates which were (117.5 cm, 231 cm, 40 cm) - for the window 1 and (117.5 cm, 88.5 cm, 0 cm) - for the window 2.

2.2. Monitoring the temperature of the solution, air and packaging surface

Temperature profiles were obtained with 45 temperature sensors (type T thermocouple copper/constantan AWG-24 and resistive thermal devices - RTDs) which were distributed within the solution, at the surface of the packaging and air. The sensors were connected to a signal conditioning system (National Instruments - Model SCXI - Hungary) and the temperature measurements were

obtained at 5 min intervals using the LabVIEW 8.5 *software*. Parallels arrangements of type-T thermocouples were distributed evenly in front, behind of the evaporator and near the tunnel floor in order to monitor the average temperature of the cooling air.

The surface temperature of the containers was measured using an infrared thermal camera (FLIR - model ETO T420 - FLIR Systems, Inc) and through two temperature sensors, which were used for calibration and adjustment of thermal images obtained. This calibration was necessary because, according to Carlomagno and Cardone [8], the energy actually detected by an infrared system (IR) depends not only the surface emissivity, but also the environmental conditions of the surroundings. According to Meinders et al. [11], the ambient contributions for the detection of radiation (e.g., reflections from hot neighboring elements), are difficult to quantify and they lead to unequivocal identifications of temperature if a calibration is not performed.

To avoid disturbances and for avoiding exposure to freezing temperatures, the infrared camera was positioned immediately outside of the freezing tunnel, in its wall, where were installed two polyethylene inspection windows (FLIR - Model IRW-3C 3"- FLIR Systems, Inc), one at the ceiling and the other one on the wall opposite to the evaporator, as shown in Fig 1. The cut out, where the inspection window and infrared camera was placed was sealed with an acrylic plate. The wet air inside the measurement chamber was partially removed by a pump vacuum (LOKRING - Model VP 340D - Vulkan Lokring, BRAZIL) to prevent the condensation in the windows and lens of infrared camera. Also, the inspection window was wiped with alcohol to prevent the air condensation due the high temperature difference between inside and outside the tunnel.

2.3. Air velocity measurements

The air velocity was measured with the aid of a hot wire anemometer (TSI - Model 9535 - TSI Incorporated, USA). The measurements were collected at 12 positions strategically and systematically located throughout the tunnel. At position, measurements were made at 6 different distances, along the horizontal and vertical direction of the air circulation, and with five replications, it yielded a total of 1440 data points. The measurements spot coordinates were z (cm) = 14 and 121; y (cm) = 5, 41, 84, 127, 170 and 213; and x (cm) = 13, 26, 39, 52, 65, 78, 157, 170, 183, 196, 209 and 222.

2.4. Settings configuration

Measurements in duplicate were made for each packaging configuration. The assembly configurations and arrangement of thermocouples are shown in Fig 2.

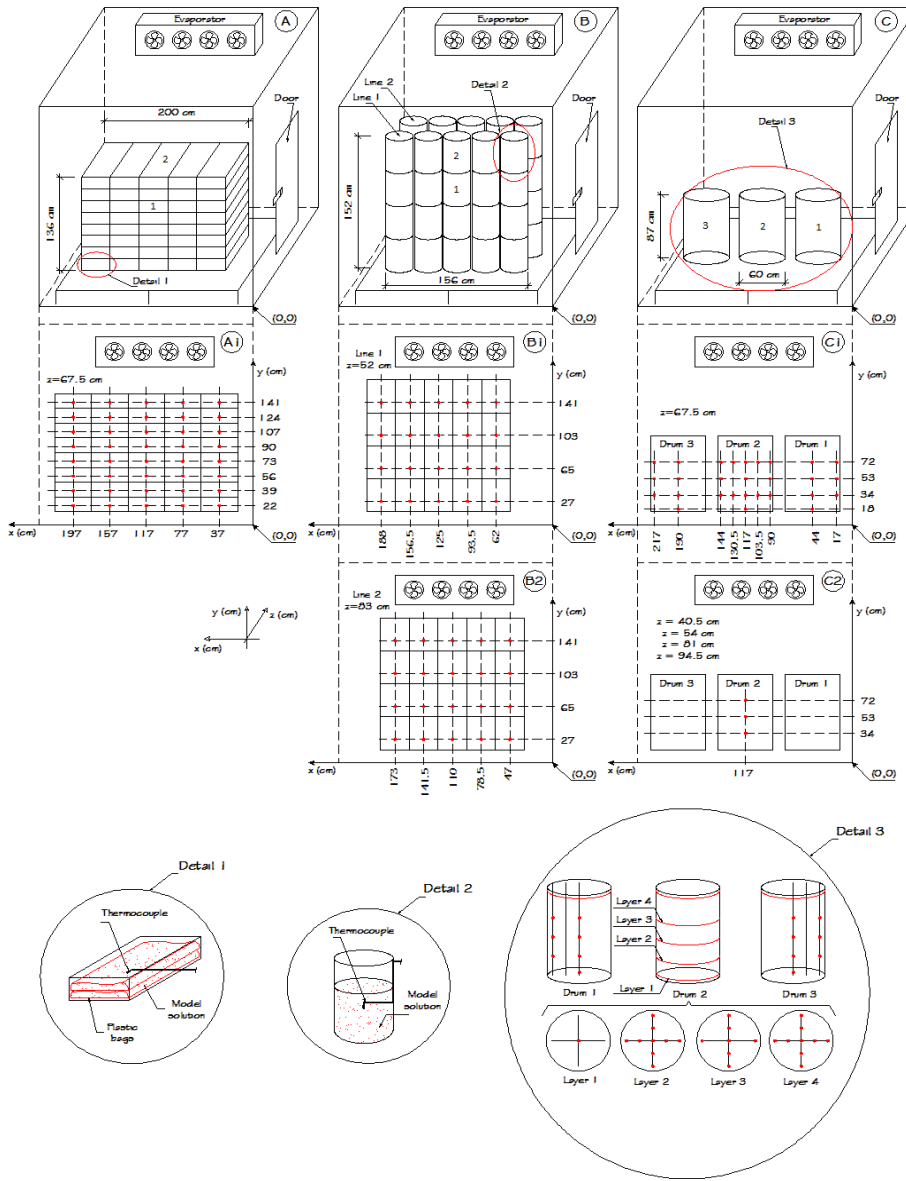


Figure 2. Configuration of the three container settings and the position coordinates of the thermocouples inside. The red dots represent the position of the temperature sensors. (A) - boxes configuration, (B) - buckets configuration and (C) - drums configuration.

For the configuration of plastic boxes and buckets, one thermocouple was installed inside each container, positioned at the center of mass of the solution. For the drum, the temperature sensors were distributed throughout the volume as shown in Fig 2 (C1, C2 and detail 3).

The containers which had their surface temperatures measured were as follow: boxes (1 - side and 2 - top), buckets (1 - side and 2 - top) and drums (2 - top and side) as shown in Fig 2. The coordinates (x, y and z) were as follow: box 1 (117.5 cm, 107.0 cm and 37.0 cm), box 2 (117.5 cm, 148.0 cm and 67.5 cm), bucket 1 (125.0 cm, 103.0 cm and 37.0 cm), bucket 2 (125.0 cm, 167.0 cm and 52.0 cm), drum 2 - side (117.5 cm, 72.0 cm and 37.5 cm) and drum 2 - top (117.5 cm, 102.0 cm and 67.5 cm).

The dimensions of the plastic buckets were 38 cm x 30 cm (height x diameter), plastic boxes of 60 cm x 40 cm x 17 cm (length x width x height) and metal drums with 87 cm x 60 cm (height x diameter). The containers were placed on top of two plastic pallets with dimensions of 15 cm x 80 cm x 120 cm (height x width x length). Placements were made covering the central part of the tunnel.

2.5. Thermophysical properties

2.5.1. Enthalpy and specific heat

Enthalpy and specific heat measurements were made using a differential scanning calorimeter (DSC) (DSC Q100, TA Instruments Inc., New Castle, DE) with a liquid nitrogen cooling system. Prior to sample measurements, the DSC was calibrated using a sapphire standard. The DSC measurements were made using 10 mg of solution which was placed in aluminum hermetically sealed pans. An empty pan was used as a reference. To evaluate the enthalpy, the

methodology consisted of establishing the sample at -25 °C, then proceeding carrying out a DSC scan at a heating rate of 2 °C/min until reaching a temperature of 25 °C. With the results of enthalpy obtained for every degree change in temperature it was possible to determine the specific heat by Eq. 1.

$$c_p = \Delta H_p / \Delta T \quad (1)$$

where:

c_p - specific heat ($\text{kJ} \cdot \text{kg}^{-1} \cdot ^\circ\text{C}^{-1}$);

ΔH_p - enthalpy variation ($\text{kJ} \cdot \text{kg}^{-1}$);

ΔT - temperature variation ($^\circ\text{C}$).

2.5.2. Freezing initiation temperature

The initial freezing point was determined by cooling curve methodology [12], considered to be one of the most simple, accurate and widely used methods to measure this parameter in foods.

2.6. Determination of the convective heat transfer coefficient (h) using conventional procedure

To evaluate the heat transfer coefficients (h), an energy balance was applied to the system as shown in equations 2 and 3. The effective temperature difference between the surface of the container (T_{ct}) and the air (T_{air}) during a time interval Δt is given by Eq. 4 [13].

$$m_{ct} c_{p_{ct}} \frac{dT_{ct}}{dt} + m_{sol} c_{p_{sol}} \frac{dT_{sol}}{dt} = \square A(T_{ct} - T_{air}) \quad (2)$$

$$h = \frac{(mc_p\Delta T)_{ct} + (mc_p\Delta T)_{sol}}{A(T_{ct} - T_{air})\Delta t} \quad (3)$$

$$T_{ct} - T_{air} = \left[\frac{T_{ct}(t) + T_{ct}(t + \Delta t)}{2} \right] - \left[\frac{T_{air}(t) + T_{air}(t + \Delta t)}{2} \right] \quad (4)$$

where:

A - heat transfer area (m^2);

m_{rp} e m_{sol} - mass of the empty container and the solution, respectively (kg);

$c_{p_{ct}}$ e $c_{p_{sol}}$ - specific heat of the container and the solution, respectively ($\text{kJ}\cdot\text{kg}^{-1}\cdot\text{°C}^{-1}$);

T_{ct} , T_{sol} e T_{air} - temperatures of the container, solution and air, respectively ($^\circ\text{C}$).

The specific heat values of the containers were $2.3012 \text{ kJ}\cdot\text{kg}^{-1}\cdot\text{°C}^{-1}$ (buckets and plastic containers of HDPE) taken according to specifications of the manufacturer and $0.444 \text{ kJ}\cdot\text{kg}^{-1}\cdot\text{°C}^{-1}$ (metal drums), according to data reported in Incropera and Dewitt [14].

According Santos et al. [13], the experimental method and energy balance used in this work is a suitable and reliable procedure for the determination of heat transfer coefficients inside industrial tunnels. The method is sensitive enough to determine spatial heterogeneities in the tunnel and is versatile with respect to the system geometry, characteristics which make it a useful and simple tool to carry out diagnostic tests in industrial plants. Cleland et al. [15] reported this method as the most common for measuring the heat transfer coefficient, however, it only provides an average surface heat transfer coefficient throughout the exposed surface.

2.7. Convective heat transfer coefficients using IR thermography

Using thermal imaging, it was possible to do a complete scan of convective coefficients on the surfaces of the containers and have a general approximation of the actual dynamics of heat transfer process. In this case, the air temperature (T_{air}) which was measured using parallel arrangements of thermocouples, solution temperature (T_{sol}) which was measured using thermocouples and container surface temperature (T_{ct}) which was measured using IR thermography were then applied in pertinent Eqs. (2 to 4).

Thermal images obtained by infrared camera were temperature corrected by calibration with temperatures measured by thermocouples arranged on the surface of the containers. This calibration was necessary because, according to Carlomagno and Cardone [8], the energy actually detected by an IR system depends not only on the emissivity coefficient of the surface under measurement but also on environmental conditions. Since the infrared camera was installed on the outside of the tunnel (room temperature) and the images were obtained using a polyethylene inspection window which its temperature was influenced by the temperatures inside and outside the tunnel, therefore there were interferences on the data obtained. Also according Meinders et al. [11] the environment contributions on the detection of radiation (for example, reflections from hot neighboring elements) are difficult to quantify and they can lead to ambiguous identifications of temperature if a calibration is not performed.

2.8. Experimental freezing time

According to Ramaswamy and Tung [16], the most frequently used definitions of the freezing time are the thermal arrest time or the duration of the freezing process from start to finish, both representing the time needed to

traverse a range of temperature. In this work the time freezing was recorded from the time that the tunnel has been connected until the moment when all thermocouples installed within the solution reached -18 °C. This temperature was chosen to be the most commonly used temperature for frozen food, commercially [17].

2.9. Energy consumption

The power consumption of the process for each configuration was measured with an electrical value transducer (KRON - Model Mult-k 120 - Brazil) that was coupled to a computer through a converter (KR-485/USB). The parameter was analyzed using the RedeMB5 e Version 5.19 *software* with serial data standard RS-485 through the Modbus protocol.

3. Results and discussion

3.1. Air velocities

Through measurements of air velocity it was possible to characterize their behavior profiles and assess differences for the three studied configurations. Contour curves were obtained through the least-squares regression technique that was implemented using StatSoft, Inc. (2007). STATISTICA (data analysis software system), version 8.0. Fig 3 shows the air velocity behavior within the tunnel in the z coordinate measuring 14 cm for the configuration of the plastic boxes (A), plastic buckets (B) and metal drums (C) relating to the measurements in the vertical direction.

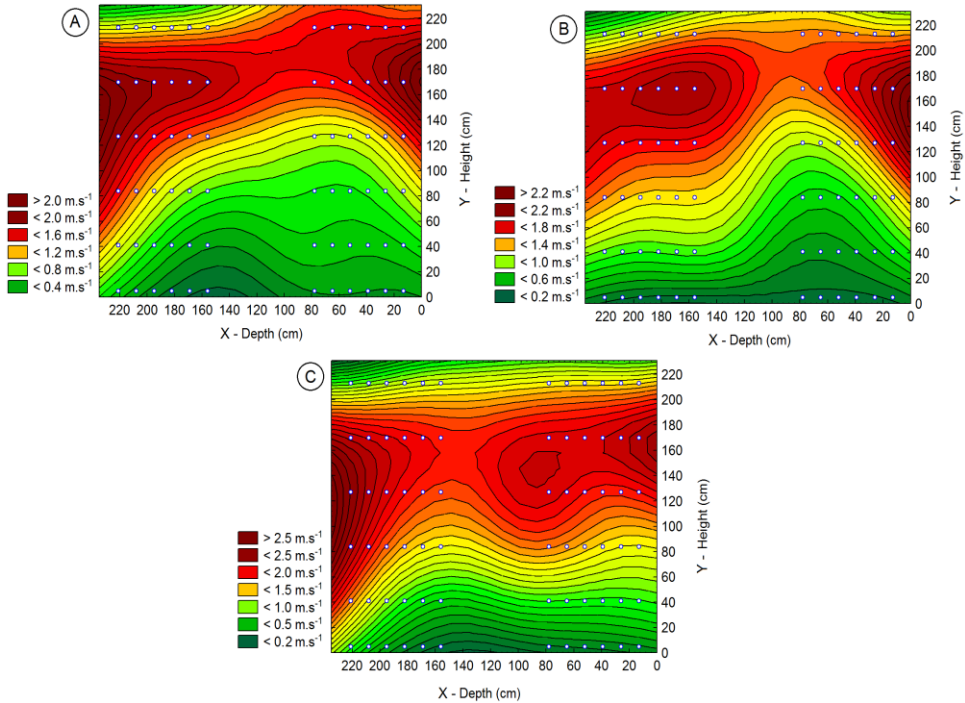


Figure 3. Profiles of the air velocity in the fixed coordinate $z - 14$ cm (evaporator outlet), and (A) - plastic boxes (B) - plastic buckets and (C) metal drums.

It can be observed from Fig 3 that for all three container types, as the height inside the tunnel increases, the air velocity becomes higher. This could be due to the positioning of the evaporator in the upper part and the presence of an empty space between the evaporator and the top of the stacks and drums. At the opposite ends ($x \sim 20$ and 220 cm) of this section, it was also observed that the profiles showed higher speeds, than the middle. This behavior may have occurred probably due to the freedom of the air passage in these places (next to the door and end of the tunnel). Since the containers were positioned in the middle of the freezer it could have allowed for the formation of preferential channels of air flow. However, for the metal drums, it can be seen that the area of higher speeds was more homogeneous across the depth of the tunnel (x

coordinate). This behavior may be because the drums have a smaller height (87 cm) compared with the stacked buckets (152 cm) and boxes (136 cm). Moreover, having space between the drums (Fig. 2), allows greater freedom for air flow not only in the ends but also between the drums. The highest air velocities observed were 2.85 m.s^{-1} ; 2.72 m.s^{-1} and 2.62 m.s^{-1} for drums, boxes and buckets, respectively.

Various works [18,2] have shown that the velocity profiles in freezing tunnels with forced air are strongly influenced by any changes in the amount of product and its distribution inside the machine. The flow can occur through preferential airflow pathways, leading to common errors in determining the freezing time and heat transfer coefficients in these devices.

3.2. Isotherm as a function of time

Figs. 4, 5 and 6 show the temperature profiles obtained during freezing of model solution for the boxes, buckets and drums, respectively.

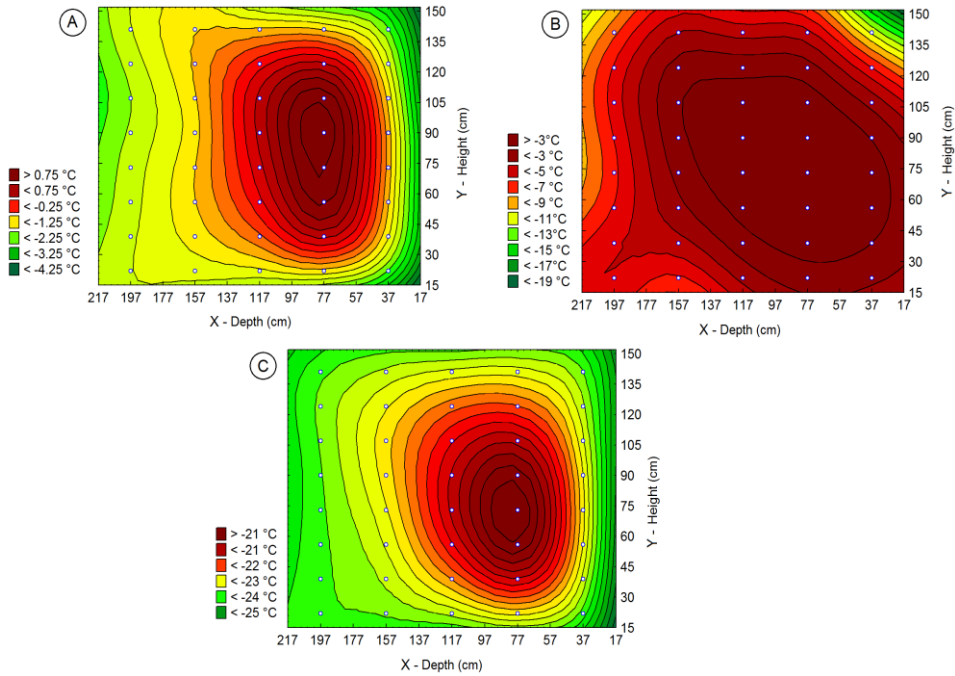


Figure 4. Isotherms obtained during freezing of solution model in plastic boxes and coordinated fixed $z = 67.5$ cm. (A) - 10 h, (B) - 30 h and (C) - 50 h.

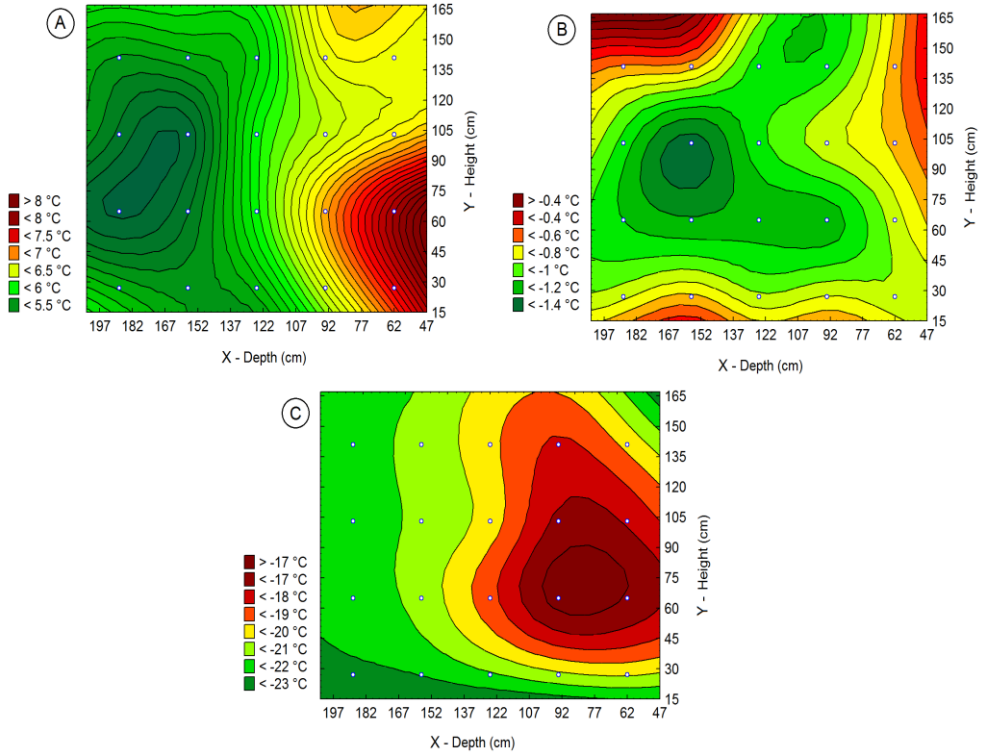


Figure 5. Isotherms obtained during freezing of solution model in buckets and coordinated $z = 52$ cm (Line 1). (A) - 10 h, (B) - 30 h and (C) - 50 h.

Figs. 4 and 5 show that the dynamic freezing occurred through a pattern of variation of temperature over time. The isotherms indicate that the movement of the freezing front traversed from the surface to center inward over the time, beginning with the outermost containers toward those located in the center of the stack. Reno et al. [18] also observed the same temperature behavior over time for guava pulp freezing in plastic boxes.

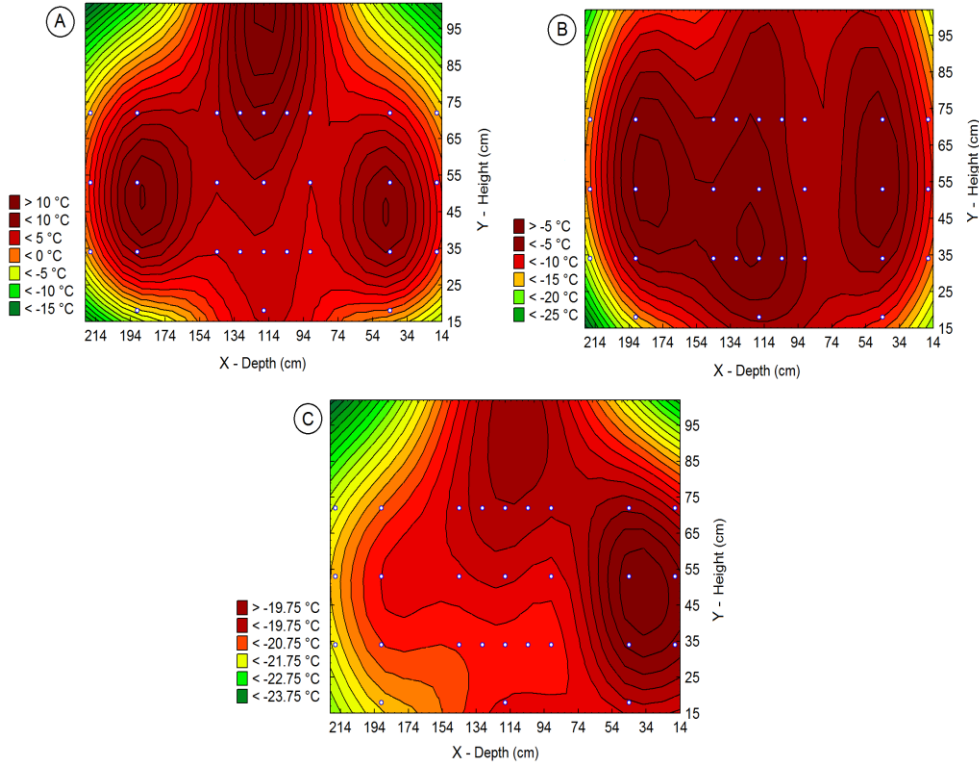


Figure 6. Isotherms obtained during freezing of solution model in metal drums and coordinated $z = 67.5$ cm. (A) - 20 h, (B) - 60 h and (C) - 100 h.

As occurred in the configuration with buckets and plastic boxes, in metal drums it was observed that the freezing occurred in the direction of the tunnel edges to the center, but unlike the first two settings, the points of higher temperatures were homogeneously located near the center geometric of the three drums, as a result of a more uniform freezing.

In Figs. 4B, 5B and 6B, corresponding to the processing time closest to the phase change of the solution, larger areas with temperatures around the freezing initiation temperature (-1.1°C) could be observed.

As well as with buckets and plastic boxes settings, in the experiments with drums probably there was also heat infiltration through the door. However,

this did not result in visual change and shifting of the thermal center at the beginning of the measurements. However, the shifting of the thermal center was observed in the end of the process (Fig. 6C). This less interference probably occurred due to the large amount of solution in the drum (200 kg) compared to 15 kg present in boxes and buckets.

Figs. 4, 5 and 6 also show that at greater depths the temperature zones observed were more homogeneous, which can be seen through the largest distance between the temperature ranges. This behavior resulted in a more uniform freezing of containers present at the end of the tunnel as compared with the containers located next to the door. They had possibly their freezing influenced by a heat load coming from external origin, infiltration through the door.

3.3. Experimental freezing time

The average time obtained was 51 h (plastic boxes), 55 h (plastic buckets) and 102 h for metal drums. For the same 600 kg of solution that was frozen, the total area of heat transfer between surface of containers and cooling fluid were approximately 6.616 m^2 , 15.739 m^2 and 17.870 m^2 for drums, buckets and boxes, respectively, which represented a ratio area per mass approximately $0.011 \text{ m}^2 \cdot \text{kg}^{-1}$, $0.026 \text{ m}^2 \cdot \text{kg}^{-1}$ and $0.030 \text{ m}^2 \cdot \text{kg}^{-1}$, respectively.

Fig. 7 shows the location of points that demanded more and less time to reach -18 °C.

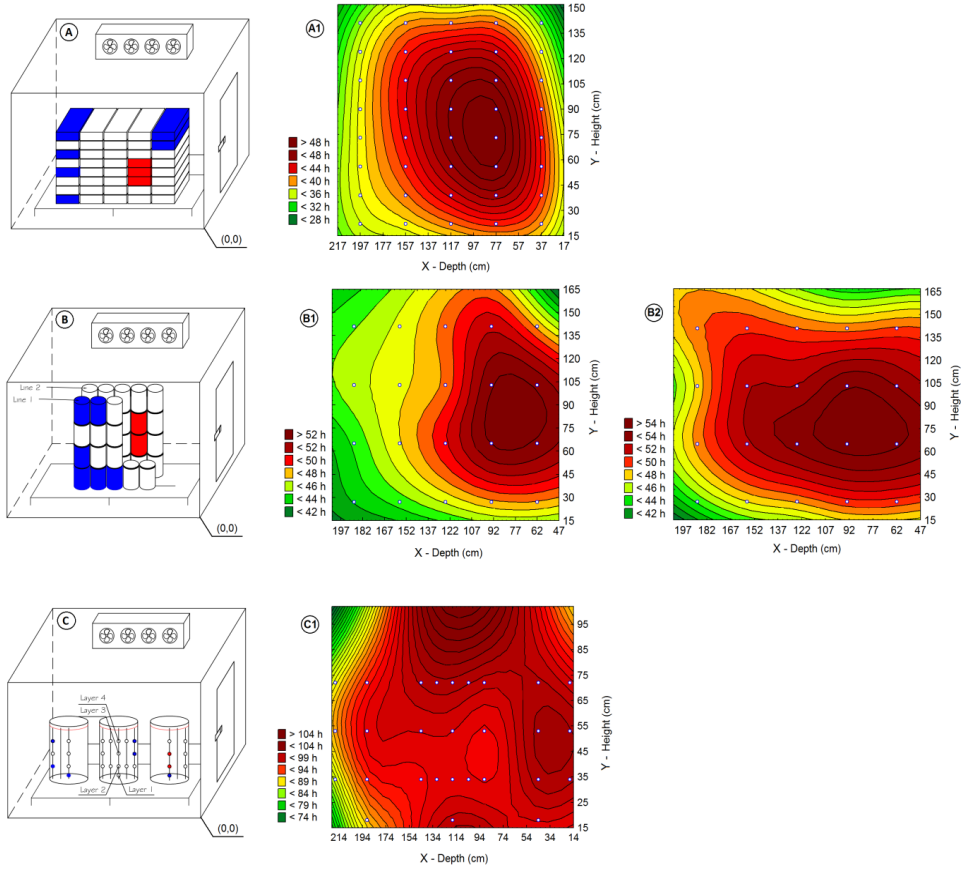


Figure 7. Location of points that demanded more (red) and less time (blue) to reach -18°C , being (A) - boxes; (B) - buckets and (C) - drums. Freezing time profiles for the boxes (A1), buckets (B1 - line 1 and B2 - line 2) and drums (C1).

Fig. 7A shows that for solutions stored in boxes longer times were observed in the samples located in the third, fourth and fifth layer of the second stack near the door, corresponding to an approximate height 56-90 cm, as it can also be observed in the freezing time profile (A1). From Fig. 4 can be seen this height range as the location of the thermal center. In the box configuration, those arranged mainly in the tunnel background required lower time to reach -18°C . They received cooling air at higher speeds (Fig. 3A), bringing as a result a

higher cooling rate. Reno et al. [18] also showed the same behavior for the guava pulp freezing in plastic boxes and freezing times longer than 50 h for samples located in the center of the tunnel in terms of their height and closest to the door. Shorter times were registered at the end of the stack and at the end of the tunnel.

Fig. 7B shows that longer freezing times with the buckets located in the second and third layers of the second line near the door, which from Fig. 5 corresponds to region with higher temperatures. As in the configuration with plastic boxes, the buckets with lowest times were found at the end of the tunnel, in line 1, which received the cooling air from the evaporator outlet (Figs. 7; B1 and B2).

For drums (Fig. 7C), layers 2 and 3, corresponding to the mass center of the drum nearest the door demanded longer freezing times, which can be evidenced by the thermal center of Fig. 6C. On the other hand, the fastest cooling occurred at locations more distributed by the three drums in comparison with the other two configurations that were concentrated in the background. This more homogeneous distribution of the freezing may be due to availability of the air passage between the drums, which led to more uniform temperatures and freezing time as shown in Fig. 6C and Fig. 7C1.

3.4. Initial freezing point

Fig. 8 shows the cooling curves of model solution in which it was possible to evaluate the initial freezing temperature (T_{if}). Measurements were performed in triplicate.

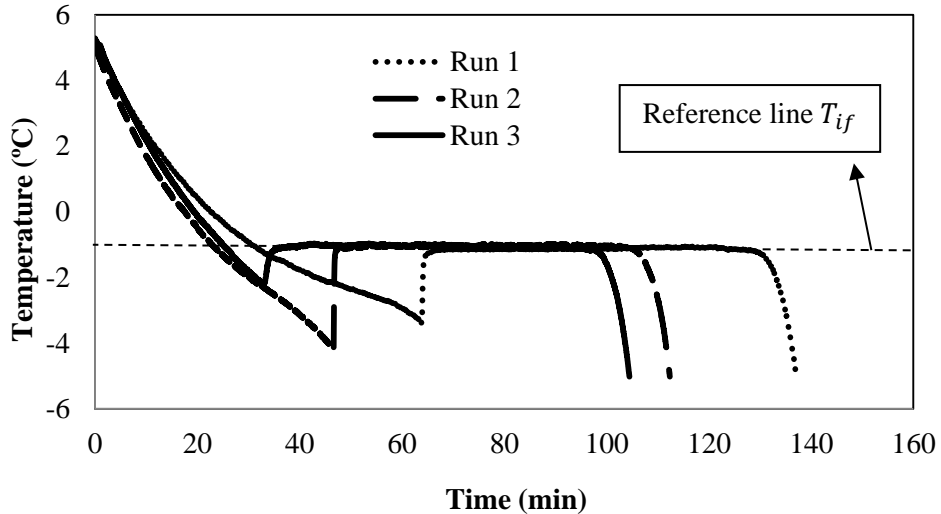


Figure 8. Cooling curves of the model solution. SC (supercooling) and T_{if} (initial freezing temperature).

All three repetitions demonstrated supercooling, defined as cooling below the initial freezing point of a sample without ice being formed. It ends when there is the formation of initial ice crystallization [12]. According to Pham [19], some degree of supercooling is observed in most food freezing processes, where the surface dips briefly below freezing point before suddenly coming up to the freezing temperature. Fellows [20] reported that the supercooling can reach up to 10 °C below the food freezing and varies according to the type of food composition and cooling rate. Rahman [12] also emphasized various factors involved in the tendency of a system to provide supercooling as temperature, cooling rate, volume and amount of solute.

The different supercooling behaviors observed were due not using the same amount of samples in three replicates and non-uniform cooling rate which did not generate losses or alterations in the determination of the initial freezing point. The freezing initiation temperature was taken as the temperature after supercooling at the beginning of substantially constant temperature plateau

characterized by a phase change of the solution. The average obtained for T_{if} was -1.1 °C with a standard deviation of 0.027.

3.4.2. Enthalpy and specific heat

By DSC analysis, polynomial equations of the form shown in Eq. 5, were adjusted to evaluate the enthalpy and specific heat of the solution in the temperature range of (-25 to 25 °C) and subsequent application in the energy balance for determining the convective heat transfer coefficient. Table 1 shows the temperature ranges, the coefficients and r^2 .

$$\text{Polynomial equation: } y = a + bT + cT^2 + dT^3 + eT^4 \quad (5)$$

Table 1 - Coefficients of the polynomial equations to evaluate the enthalpy ($\text{kJ} \cdot \text{kg}^{-1}$) in different temperature ranges within the freezing process.

Temperature (°C)	Coefficients					R^2
	a	b	c	d	e	
$25 > T_{if}$	247.634	6.404	-0.511	0.030	-5.796E-4	0.998
$-25 \leq T < T_{if}$	291.390	52.122	4.261	0.166	2.416E-3	0.999

3.5. Convective heat transfer coefficients

To calculate the average convective coefficient, the values used were only those obtained in the phases of precooling and tempering period, and values obtained during the phase change were discarded due to the sharp increase in specific heat (latent heat release), which could generate unambiguous results in the convective heat transfer coefficient. According Belchior et al. [21], below the initial freezing point, the heat transfer coefficients values go through extreme variations and cannot be deduced properly using the energy balance applied in this work. This is because during the change phase, heat is transferred not just

between air and solution, but also between the solutions of the container. Fig. 9 shows the distribution of local convective heat transfer coefficients and temperature profiles (solution and air) obtained during the freezing of the model solution in the boxes (A), buckets (B) and drums (C). The acquisitions of the temperature data at the container surface and inside the solution were related to the box 2, bucket 2 and drum 2, as shown in Fig. 2.

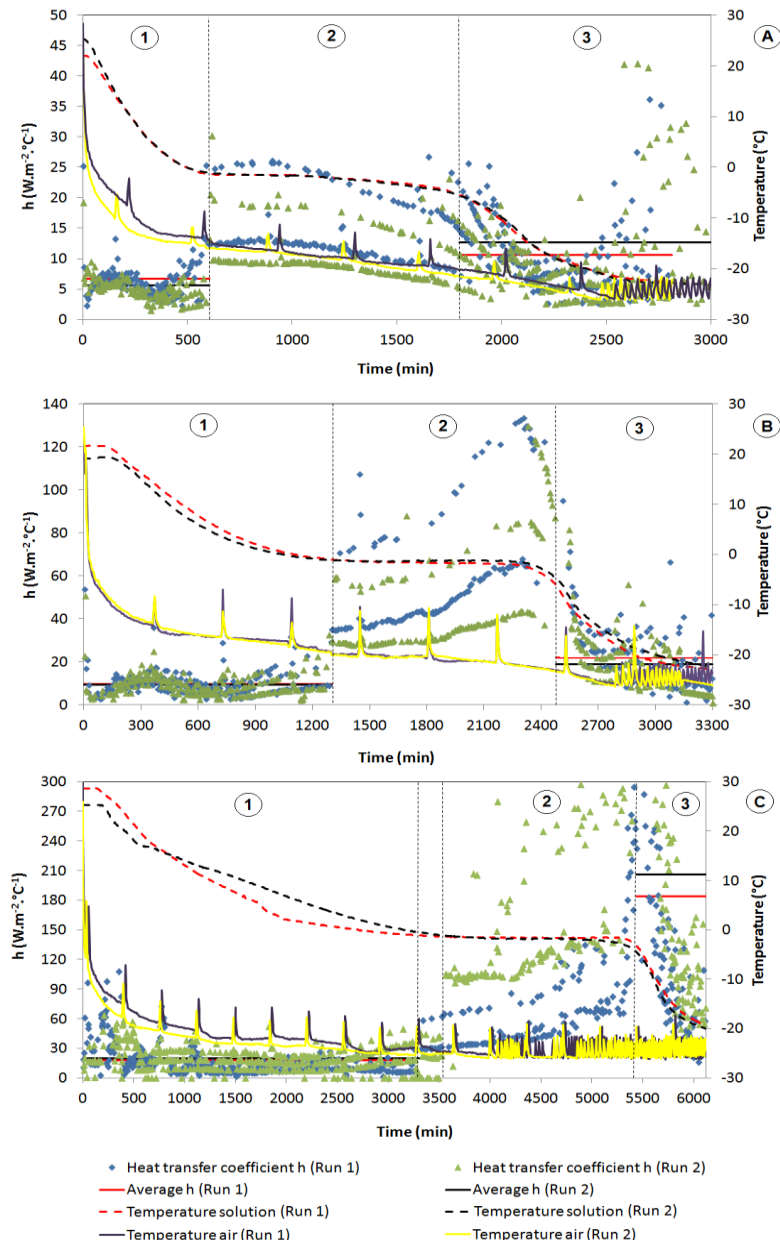


Figure 9. Temperature profiles (solution and air), local convective heat coefficients and their average (before and after freezing the solution). (A) - boxes, (B) - buckets and (C) - drums. (1) - precooling period, (2) - phase change period and (3) - tempering period.

Fig. 9 shows that the distribution of the local convective heat coefficients (h) throughout the freezing process was not constant. Variations and different intensities of scatter were observed for the different packaging configurations and for the different periods during the freezing process (precooling period, phase change and tempering period). According to Belchior et al. [21], the dispersions may be associated with the use of difference of mean temperature (Eq. 4) to calculate the energy balance. Santos et al. [22] also worked with average heat transfer coefficients while studying the heat transfer during the freezing of poultry cuts in continuous convective air blast tunnels and did also note dispersions in the values of the coefficients.

During the measurements of air velocity inside the tunnel, fluctuations were observed due to the turbulent flow. This eventually had implications on the local convective coefficients of heat transfer. According Pham et al. [23], as the heat transfer rate depends on the air flow conditions, local variations in the coefficients are expected along the surface. Still according to Kondjoyan [24], the food arrangements include a large number of rows subjected to surrounding air flows, leading normally a turbulent flux. Becker and Fricke [4] claim the velocity of fluid through the product is the most significant factor influencing the surface heat transfer coefficient. Thus, large differences in the heat transfer coefficient (h) can be explained by local differences in air velocity.

Among the three settings, the scatters in h were more pronounced for the drums (Fig. 9C), which may be explained by the higher air velocity detected in this configuration, leading to increased turbulence inside the tunnel and consequently large fluctuations in the local h .

Table 2 shows the average convective coefficients (precooling and tempering period) on the side and top of each studied configuration with the corresponding standard deviation.

Table 2 - Average convective coefficients (precooling and tempering period) on the side and top of each studied configuration with the respective standard deviation (SD) and coefficient of variation (CV).

Configuration	Average convective coefficients ($\text{W} \cdot \text{m}^{-2} \cdot ^\circ\text{C}^{-1}$) (SD - CV)			
	Side		Top	
	Precooling period	Tempering period	Precooling period	Tempering period
Boxes	200 (± 3.91 - ± 0.02)*	210 (± 24.7 - ± 0.12)*	6.31 (± 0.71 - ± 0.11)	11.6 (± 1.52 - ± 0.13)
Buckets	6.23 (± 0.05 - ± 0.01)	14.2 (± 2.35 - ± 0.17)	9.57 (± 0.18 - ± 0.02)	21.3 (± 3.61 - ± 0.17)
Drums	15.5 (± 0.63 - ± 0.04)	180 (± 3.43 - ± 0.02)*	18.5 (± 1.39 - ± 0.08)	195 (± 15.6 - ± 0.08)*

(*) - values incompatible with the reality of an air cooling.

In the configuration of the boxes, the surface temperature of the box 1 (side) matched the air temperature in the first few measurements (still at the precooling phase), which eventually generated a cooling rate ($T_{ct} - T_{air}$) very low, causing convective coefficients data too high and incompatible with the reality of an air cooling. This may have occurred due to the thermocouple positioning on the lateral surface of the box. Since the box had small holes and dimples on its surface, the thermocouple was not in a full contact with the packaging, being partially in contact with air holes. This therefore did not allow a complete transfer of heat between thermocouple and packaging leading to a cooling rate measurement ($T_{ct} - T_{air}$) very low. Belchior et al. [21] has observed similar behavior between the temperature history of sensors installed in boxes and the air temperature by working with passion fruit pulp contained in high-density polyethylene (HDPE) boxes and frozen without and with airflow induction.

The average values of the coefficients were different when measured on the side and on top of each configuration. The top values have shown have always been higher. This difference may again be related to the highest values of air speed (Fig. 3) in the highest y-coordinate locations in the tunnel. Through

Fig. 2 in which can view the positioning heights within the tunnel in which the coefficients of Table 2 were obtained, and comparing these heights with the corresponding air velocity (Fig. 3), it can be observed a direct correlation, which the highest coefficients corresponded to higher speed values of the air.

Regarding to the precooling and tempering periods, it has been observed that the greater values at the average convective heat coefficient occurred at the tempering period, for all the three packaging configurations, as shown in Table 2, mostly because of carryover effects of the phase change period. Such behavior can be explained in part by the fact that, because the solution already be completely frozen, the water present is in the form of ice that has a higher thermal conductivity than that of liquid water, resulting in better heat transfer within the solution, which therefore generates higher convective heat transfer coefficient values between the surface and the cooling air. According to Ramaswamy and Tung [25], below the freezing point, thermal conductivity values show a large scattering with temperature, and Carson [26] claims that the conductivity of the ice is about four times that of liquid water.

During the tempering period a larger scatter was also observed for the local heat transfer coefficients as compared to the precooling period. According to Belchior et al. [21], the dispersions may be associated with air temperature fluctuations caused by the defrosting at specific programmed time intervals. In freezing tunnel used in this work, the defrosting interval occurred every 360 min, which can easily be observed in Fig. 9, until approximately the processing times of 2500 min (boxes configuration), 2800 min (buckets configuration) and 4000 min (drums configuration). After these periods of processing, the defrosting continues occurring every 360 min, but it is also observed an on/off cycle each 20 min, due to the fact that there is no more thermal load because the air temperature has already reached -25 °C (fixed working temperature). At that on/off cycle can be related to a greater scatter of coefficients (h) and consequent

increase in their average for all studied configurations (Fig. 9). However in metal drums, the average of the coefficients h were incompatible with an air cooling. One possible explanation is that the on/off cycle every 20 min covered the entire tempering period, unlike the settings of boxes and buckets. Furthermore, the significantly longer freezing time for the solution in the drums has made the temperature difference between the surface and the air ($T_{ct} - T_{air}$) be relatively lower when compared with buckets and drums, causing high convective coefficients data.

Comparing the three configurations, Fig. 9 and Table 3 show that the average values of convective heat transfer coefficients were greater in the drum configuration, followed by buckets and boxes, which again can be related with the intensity of air velocity (Fig. 3). Kondjoyan et al. [24] found the h value of $8.3 \text{ W.m}^{-2}.^{\circ}\text{C}^{-1}$ for cylinders with $H/D = 6$ and speed of 1 m.s^{-1} . Hu and Sun [27] found that the h value varied between 8 and $14 \text{ W.m}^{-2}.^{\circ}\text{C}^{-1}$ for cylindrical packaging of ham with medium air speed of 1.33 m.s^{-1} .

The evaluation of surface temperature using thermocouples in this work permitted the measurement of only one value for the heat transfer coefficient. Thermal imaging was used to evaluate complete distribution of the heat transfer coefficient over the entire packaging surface as shown in Fig. 10.

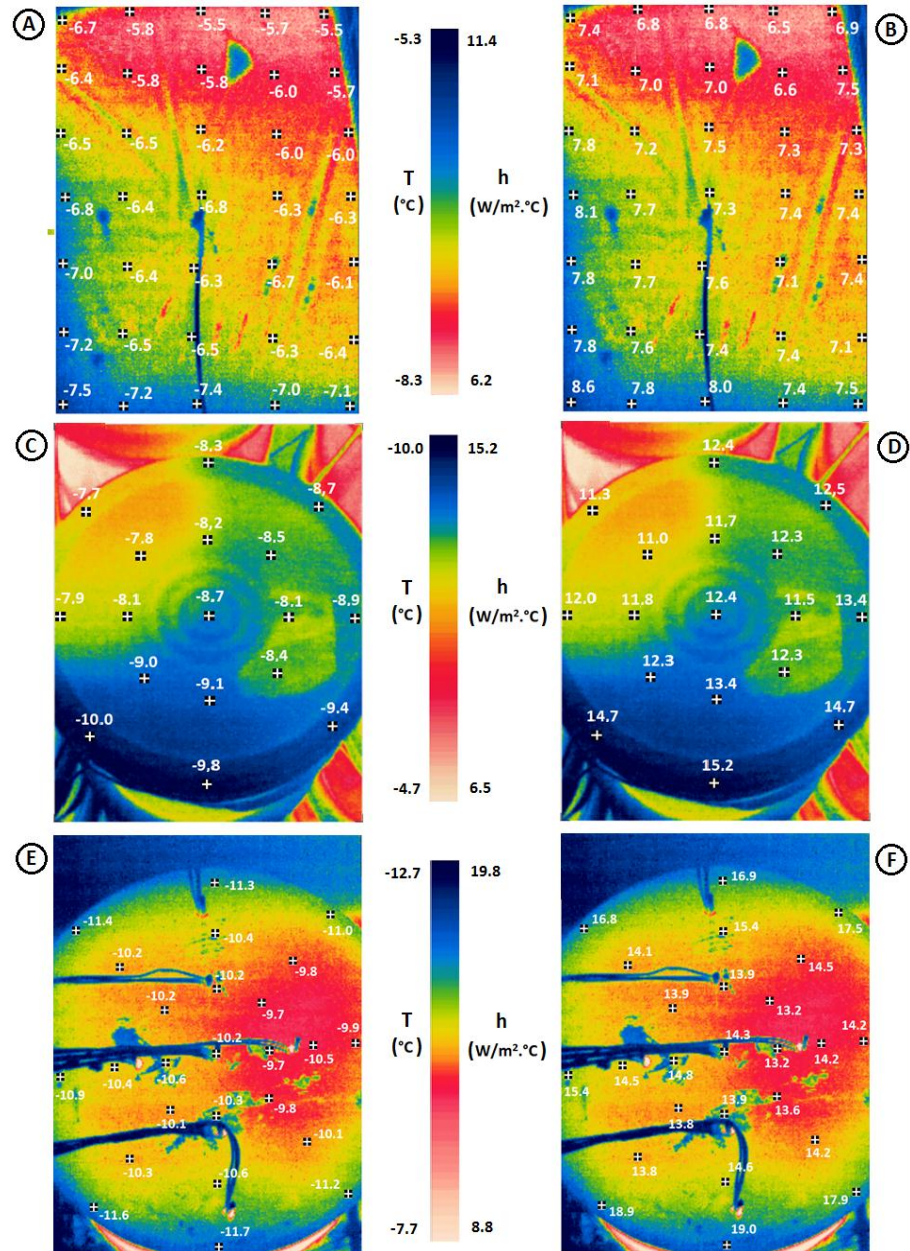


Figure 10. Evaluation of the temperature distribution and heat transfer coefficients on the surface for different containers. Boxes (A and B) and buckets (C and D) and drums (E and F). The processing times were: 8.3 h (box), 5.5 h (buckets) e 8.0 h (drums).

Fig. 10 shows that for all packaging configurations, lower temperatures (A, C e E) were observed on the side opposite to the evaporator air outlet, which shows the effect of greater cooling air speeds in order to provide a more rapid drop in temperature. Consequently, larger heat transfer coefficients corresponded to points of lower temperatures.

The temperature distribution Fig. 10 (A, C and E) on the surfaces of the boxes, buckets and drums did not appear homogeneous. Variations of approximately 2.0, 2.3 and 2.0 °C were observed, respectively, with the three configurations. It seems that differences in distribution of heat transfer coefficients on the packaging surface were actually caused by variations in temperature, even in the metal drum, that by having a high thermal conductivity, its resistance to heat transfer could be neglected and the average \bar{h} value could be considered equal to its entire surface. According to Ghisalberti and Kondjoyan [1], when the Biot number is very small $Bi < 0.1$ (sample of small dimensions and high heat conductivity), the temperature is uniform everywhere at the surface and inside the sample. In this case it is considered a average transfer coefficient for all the surface.

The variations in heat transfer coefficients were approximately 2.1, 4.2 and $5.8 \text{ W.m}^{-2}.\text{°C}^{-1}$, referring to the packaging of boxes (Fig. 10B), buckets (Fig. 10D) and drums (Fig. 10F), respectively.

3.7. Energy consumption

Table 3 shows the values concerning the energy expenditure for processing 600 kg of solution, the average time, total area of heat transfer surface of containers, the ratio area per mass in the three configurations studied and the standard deviation.

Table 3 - Average processing time, active energy, total area of heat transfer and ratio area per mass during the freezing process of 600 kg of solution, as well as the respective standard deviation (SD) and coefficient of variation (CV).

Configuration	Processing time (hours)	Active energy (kWh)	Total area (m ²)	Ratio area per mass (m ² .kg ⁻¹)
Boxes	51 ($\pm 2.91 - \pm 0.057$)	225 ($\pm 12.77 - \pm 0.057$)	17.87	0.030
Buckets	55 ($\pm 0.14 - \pm 0.003$)	248 ($\pm 0.46 - \pm 0.002$)	15.74	0.026
Drums	102 ($\pm 0.71 - \pm 0.007$)	437 ($\pm 0.28 - \pm 0.001$)	6.62	0.011

Table 3 shows that the lowest energy consumption was observed for the solutions packaged in boxes (225 kWh) and the more energy intensive configuration was the metal drum with an active energy consumption of 437 kWh due to the longer time required to freeze completely the samples.

It was observed that the energy demand had a direct relationship with freezing time and the area available for heat exchange is a major contributing factor to the differences in values observed in freezing times and power consumption. Comparing boxes and drums configuration, there was a increase of 96% (processing time) and 94% (energy consumption) when the total area of heat transfer was reduced almost 3 times.

4. Conclusions

In this work it was possible to study the dynamics of heat transfer process during the freezing of fruit juice model solutions in a freezing tunnel. With the different commercial packaging and settings it was possible to evaluate the distribution of air velocity profiles and temperature throughout the product and inside the equipment.

With the three analyzed packaging configurations, air velocity profiles in the freezing tunnel showed similarity, with highest values achieved at higher heights of position (y coordinate) and at the opposite ends (x coordinate).

Temperature profiles during the freezing of the solutions also showed relatively similarity with all three configurations. The isotherms demonstrated that the freezing front moved from the peripheral regions of the stacks and drums toward the thermal center which shifted closer to the door due the influence of heat load sources by infiltration from the external environment.

The freezing time was significantly higher with metal drums (almost double) than in plastic boxes and buckets settings, demonstrating that the choice of packaging is an important and significant point to optimize the cooling process.

In terms of energy consumption the type of packaging used and the area available for heat exchange can lead to great demands and make the expensive process. Freezing in metal drums consumed 94% more energy compared to the plastic boxes and 76% more compared to plastic buckets.

The main result of this paper was the experimental method itself. The proposed methodology of infrared thermography (IR) proved useful in the study of heat transfer coefficients, allowing their mapping on the entire surface of the packaging, without the necessity of direct contact with the product. Its use can therefore be an alternative technique and with significant advantage over the

traditional procedure with the use of thermocouples for evaluating convective heat transfer coefficients during thermal processes in food industry practices.

Acknowledgements

The authors wish to thank the Fundação de Amparo à Pesquisa do Estado de Minas Gerais (FAPEMIG- Brazil), Conselho Nacional de Desenvolvimento Científico e Tecnológico (CNPq - Brazil), and Coordenação de Aperfeiçoamento de Pessoal de Nível Superior (CAPES - Brazil) for financial support for this research.

References

- [1] Ghisalberti L, Kondjoyan A. A thermographic method to map the local heat transfer coefficient on the complete surface of a circular cylinder in an airflow. International Journal of Thermal Science 2001;40:738-752.
- [2] Resende JV, Torres ME, Silveira Junior V. Non-uniform heat transfer during air-blast freezing of a fruit pulp model in multilayer boxes. Food Bioprocess Technol 2013;6:146-159.
- [3] Amarante A, Lanoiselé JL. Heat transfer coefficients measurement in industrial freezing equipment by using heat flux sensors. Journal of Food Engineering 2005;66: 377-386.
- [4] Becker BR, Fricke BA. Heat transfer coefficients for forced-air cooling and freezing of selected foods. International Journal of Refrigeration 2004;27:540-551.
- [5] Resende JV, Neves Filho LC, Silveira Junior V. Escoamento de ar através de embalagens de polpa de frutas em caixas comerciais: efeitos sobre os perfis de

velocidade em túneis de congelamento, Ciência e Tecnologia de Alimentos 2002;22:184-191.

- [6] Becker BR, Fricke BA. Determination of heat transfer coefficients for the freezing of foods. In: Proceedings of the 21st international congress of refrigeration, Washington, DC; 2003. International Institute of Refrigeration.
- [7] Cleland AC, Ozilgen S. Thermal design calculations for food freezing equipment: past, present and future. International Journal of Refrigeration 1998;21:359-371.
- [8] Carlomagno GM, Cardone G. Infrared thermography for convective heat transfer measurements. Exp Fluids 2010;49:1187-1218.
- [9] Gowen AA, Tiwari BK, Cullen PJ, McDonell K, O'donell CP. Applications of thermal imaging in food quality and safety assessment. Trends in Food Science & Technology 2010;21:190-200.
- [10] Ibarra JG, Tao Y, Walker J, Griffis C. Internal temperature of cooked chicken meat through infrared imaging and time series analysis. Transactions of ASAE 1999;42:1383-1390.
- [11] Meinders ER, van der Meer ThH, Hanjali K, Lasance, CJM. Application of infrared thermography to the evaluation of local convective heat transfer on arrays of cubical protrusions. Int. J. Heat and Fluid Flow 1997;18:152-159.
- [12] Rahman MS. Food properties handbook. 2. ed. Boca Raton: CRC Press; 2008.
- [13] Santos CA, Carciofi BAM, Dannenhauer CE, Hense H, Laurindo JB. Determination of heat transfer coefficient in cooling-freezing tunnels using experimental time-temperature data. Journal of Food Process Engineering 2007;30:717–728.
- [14] Incropera FP, Dewitt DP. Fundamentos de transferência de calor e de massa. 5th ed. São Paulo: LTC; 2003.

- [15] Cleland DJ, Cleland AC, Jones, RS. Collection of accurate experimental data testing the performance of simple methods for food freezing time prediction. *Journal of Food Process Engineering* 1994;17:93-119.
- [16] Ramaswamy HS, Tung MA. A review on predicting freezing times of foods. *Journal of Food Process Engineering* 1984;7:169-203.
- [17] Delgado AE, Sun DW. Heat and mass transfer models for predicting freezing processes - a review. *Journal of Food Engineering* 2001;47:157-174.
- [18] Reno MJ, Resende JV, Peres AP, Giarola TMO, Prado MET. Heat transfer and energy consumption in the freezing of guava pulp in large containers. *Applied Thermal Engineering* 2011;31:545-555.
- [19] Pham QT. Modelling heat and mass transfer in frozen foods: a review. *International Journal of Refrigeration* 2006;29:876-888.
- [20] Fellows PJ. *Food Processing Technology - Principles and Practice*. Third edition. New York: CRC Press; 2009.
- [21] Belchior NC, Giarola TMO, Resende JV. Effects of airflow induction on heat transfer and energy consumption while freezing passion fruit pulp in stacked boxes. *Energy Efficiency* 2014;7:777-790.
- [22] Santos CA, Laurindo JB, Silveira Júnior V, Hense H. Influence of secondary packing on the freezing time of chicken meat in air blast freezing tunnels. *Ciênc. Tecnol. Aliment.* 2008;28:252-258.
- [23] Pham QT, Trujillo FJ, Mcphail N. Finite element model for beef chilling using CFD - generated heat transfer coefficients. *International Journal of Refrigeration* 2009;32:102-113.
- [24] Kondjoyan A. A review on surface heat and mass transfer coefficients during air chilling and storage of food products, *International Journal of Refrigeration* 2006;29:863-875.
- [25] Ramaswamy HS, Tung MA. Thermophysical Properties of Apples in Relation to Freezing. *Journal of food science* 1981;46:724-728.

- [26] Carson JK. Review of Effective Thermal Conductivity Models for Food. International Journal of Refrigeration 2006;29:958-967.
- [27] Hu Z, Sun DW. Predicting local surface heat transfer coefficients by different turbulent k- ϵ models to simulate heat and moisture transfer during airblast chilling. International Journal of Refrigeration 2001;24:702-717.